Sensor and Simulation Notes

Note 463

January 2002

Results of Optimization Experiments on a Solid Reflector IRA

Leland H. Bowen and Everett G. Farr
Farr Research, Inc.

Carl E. Baum, Tyrone C. Tran, and William D. Prather
Air Force Research Laboratory, Directed Energy Directorate

Abstract

We present here the results of modifications and experiments on four versions of a solid 18-inch diameter reflector IRA. We describe numerous experiments to increase the effective gain, reduce crosspol coupling, reduce sidelobes, and reduce TDR reflections at the end of the feed arms. We investigate reducing the crosspol by improving antenna symmetry with dummy cables. We also investigate the addition of a ground plane to reduce the crosspol and increase mechanical sturdiness. We also investigate adding absorber around the rim of the reflector to reduce the sidelobes. Finally, we investigate the use of a radome manufactured by MRC.

This work was funded in part by the Air Force Office of Scientific Research, Alexandria, VA, and in part by the Air Force Research Laboratory, Directed Energy Directorate, under contract F29601-00-C-0045.

I. Introduction.

We describe here the development of a solid reflector Impulse Radiating Antenna (IRA) through a series of modifications and improvements. We describe both the theoretical basis for the modifications and the experimental results. The antenna used for this series of experiments has an 18-inch diameter spun aluminum reflector with an *F/D* of 0.5. We develop in this note improved versions of the IRA-1 and IRA-2 over those previously described in [9] and [3], respectively. We go on to develop new designs for the IRA-3 and IRA-4, in an attempt to further increase gain, reduce crosspol, reduce sidelobes, and improve mechanical sturdiness. We document how well a number of new ideas work to improve antenna performance.

We begin with the IRA-1, which has feed arms located in the traditional position of ±45° from the vertical. The modifications to the IRA-1 from [9] include improving the symmetry about the vertical E plane, tuning the resistors for low reflection, and strengthening the feed point. Two previous IRAs with feed arms at ±45° had extremely flat TDRs at the resistors, so we thought it would be useful to investigate how flat a TDR we could achieve with an 18-inch diameter reflector. One of these earlier designs was a collapsible IRA with four-foot radius [3], and another was a six-foot diameter IRA with solid reflector [11].

Next, we consider the IRA-2, which has feed arms positioned at ±30° to vertical, in order to increase gain and decrease crosspol. The design of the IRA-2 is based on theory developed by J. Scott Tyo [1] and Carl Baum [2]. The design we tested here was previously described and characterized in [3], but we found problems in the earlier data that are corrected here. This allows us to compare the performance of the IRA-2 to both the IRA-1 and IRA-3.

Next, we consider the IRA-3, with a ground plane in the horizontal plane of symmetry, to reduce the crosspol and increase the sturdiness of the antenna. We performed a large number of experiments on the IRA-3 to improve the feed point design and the load resistor configuration. We also added a radome manufactured by Mission Research Corporation (MRC) to protect the antenna.

Finally, we repositioned the feed arms so their outer edge aligned with the outer edge of the reflector, resulting in the IRA-4. This was done to reduce the sidelobes, which might be enhanced by the high fields near the reflector rim. For the same reason, we also placed microwave absorber foam around the edge of the reflector. This was studied on both the IRA-3 and IRA-4.

The technique for characterizing the antennas is the same as that used previously in [3]. The antenna measurements presented here were made using the outdoor time domain antenna range at Farr Research. The source antenna was a Farr Research Model FRI-TEM-01-50 sensor and the IRA under test was the receiver. The distance between the apertures was 10 m. The sensor characteristics are given in [4]. The time domain measurements are processed using the procedure given in [6], which is a simplification of the earlier procedure given in [5]. The effective gain was calculated from the raw data as described in [6].

We also investigate the effects of improving the symmetry of the antenna, in order to reduce the crosspol coupling to the antenna. Carl Baum has shown in [7] that by carefully maintaining the symmetry of the antenna, the crosspol should be eliminated. We improved the symmetry of our antennas by adding dummy cables on the opposite side of the vertical plane of symmetry. We also redesigned our support structure near the feed point so it would be more symmetrical.

Next, we investigated eliminating the portion of the aperture field that contributes negatively to the radiated field. For all IRAs there is an area of the parabolic reflector between the feed arms where the electric fields have the incorrect polarity. This region is negligible in the IRA-1 through IRA-3, but it is significant in the IRA-4. A sketch of this region is shown in Figure 1.1 for the electrode configuration of the IRA-4 (±30°, Z_0 = 200Ω) [8]. To address the problem, we investigated covering the relevant region with microwave absorber foam in the experiments where absorber foam is used to reduce the sidelobes.

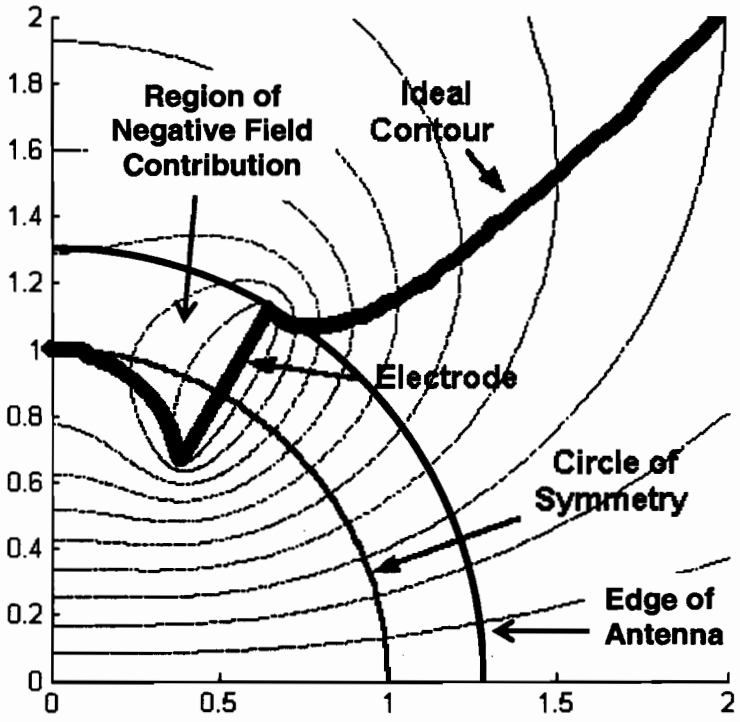

Figure 1.1. Sketch of the aperture fields of one-quarter of an IRA reflector.

A final improvement to the antenna design is due to an improved splitter. The splitter is the portion of the balun that splits the 50-ohm input into two 100-ohm transmission lines. Improvements in the splitter were incorporated into the IRA-4, resulting in much smaller reflections.

We begin now with a discussion of improvements made to the IRA-1, with feed arms located at ±45° to vertical.

II. IRA-1.

We investigate here an improved IRA-1, with feed arms at ±45°, building on our earlier work in [9]. We looked at this because earlier papers [3, 11] achieved extremely flat TDRs with a similar configuration. Such flat TDRs might be useful in radar applications. Our improvements included modifications to the feed point and to the resistors.

The IRA-1 has a 457 mm (18 in.) diameter aluminum reflector with an *F/D* of 0.5. The feed arms for this case have an included angle of 13.6°. For the original IRA-1 [9], the load resistance at the end of each feed arm was made up of two 400-ohm High Voltage Resistors (HVRs) mounted in parallel on a small circuit card. The load resistors were manufactured by HVR Advanced Power Components. For the improved IRA-1, shown in Figure 2.1, the high-voltage resistors have been replaced with a distributed resistance. The HVRs were originally used so that the antenna could be driven with a high voltage pulser. The new load configuration has five resistor strings in parallel. Each string has three resistors in series for a total of 1000 ohms in each string. Experiments using a Grant Applied Physics model HYPS source, with peak output greater than 3 kV, showed that the standard 2-watt metal film resistors could operate safely at 1.5 kV per resistor, due to the short duration of the pulse. The RF characteristics of the improved IRA-1 are shown in Figures 2.2–2.6. In addition to the distributed load resistors, this version of the IRA-1 has a more symmetric Teflon support at the feed point. It also has a dummy cable on the upper left feed arm to improve the symmetry about the vertical symmetry plane. Improving the symmetry in this way was intended to reduce the crosspol, as shown by Carl Baum in [7].

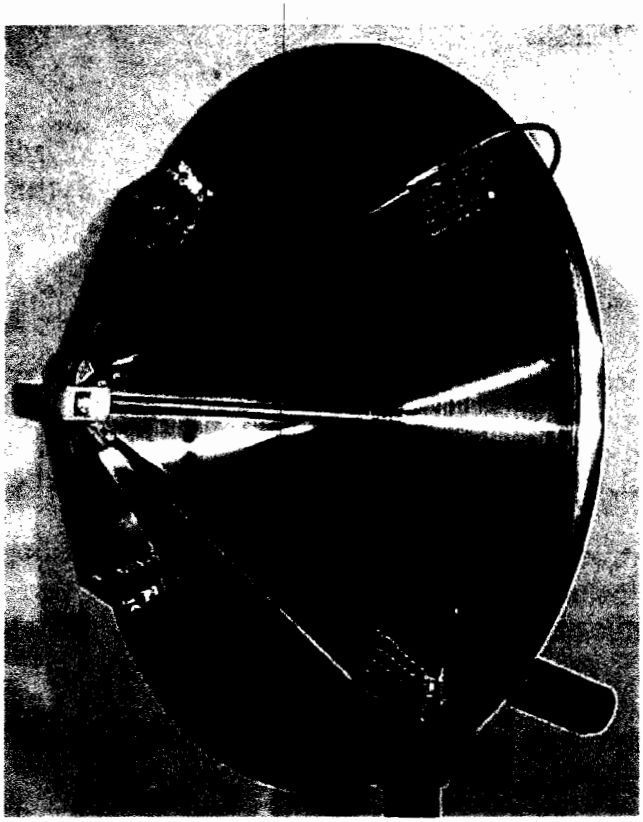

Figure 2.1. IRA-1 (Feed arms at ±45°).

In Figure 2.2 we show the TDRs of both the original and improved versions of the IRA-1. The original IRA has a large dip in the impedance at the load resistors. The distributed load resistance reduces this dip and greatly improves the TDR of the antenna. The normalized impulse response is shown in Figure 2.3. The aperture height for this antenna is 124 mm, which is 12% better than the original IRA-1.

In Figures 2.4 – 2.5, we show the effective gain of the IRA-1 on boresight for both the copol and crosspol configurations. In Figure 2.5 we see that there is considerable improvement in the crosspol rejection for the new IRA-1, as well as some improvement in the gain over most of the frequency range. The normalized antenna patterns are shown in Figure 2.6.

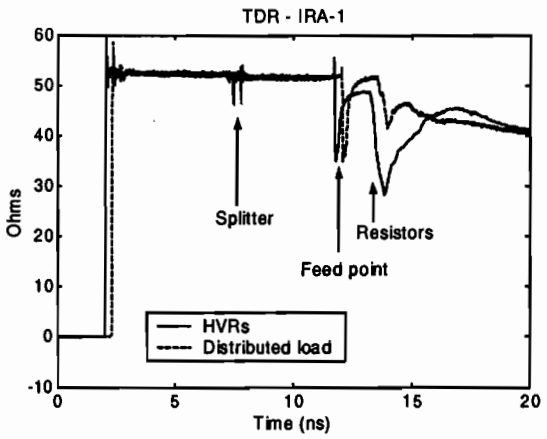

Figure 2.2. TDR of the IRA-1.

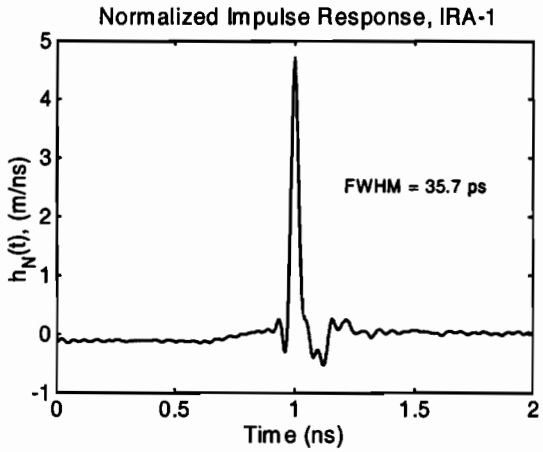

Figure 2.3. Normalized Impulse Response.

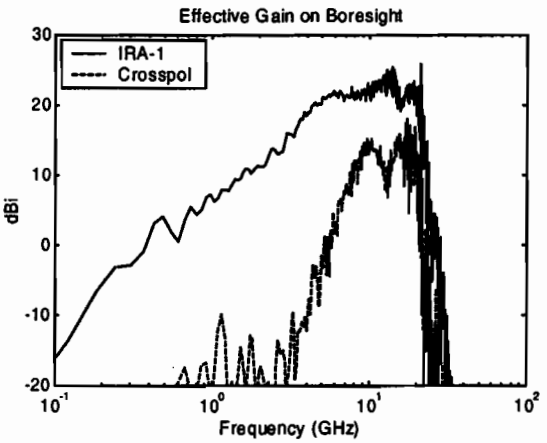

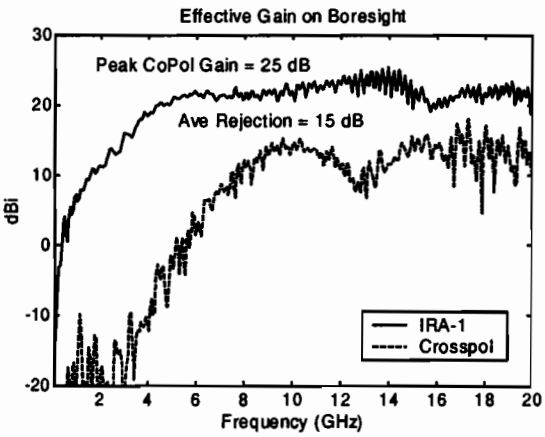

Figure 2.4. Effective gain of the IRA-1 on boresight for copol and crosspol.

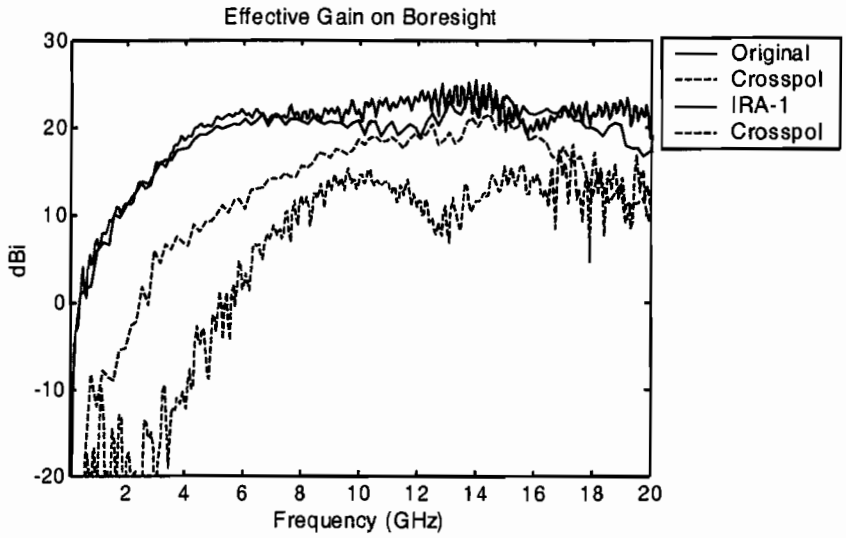

Figure 2.5. Comparison of the original and improved IRA-1.

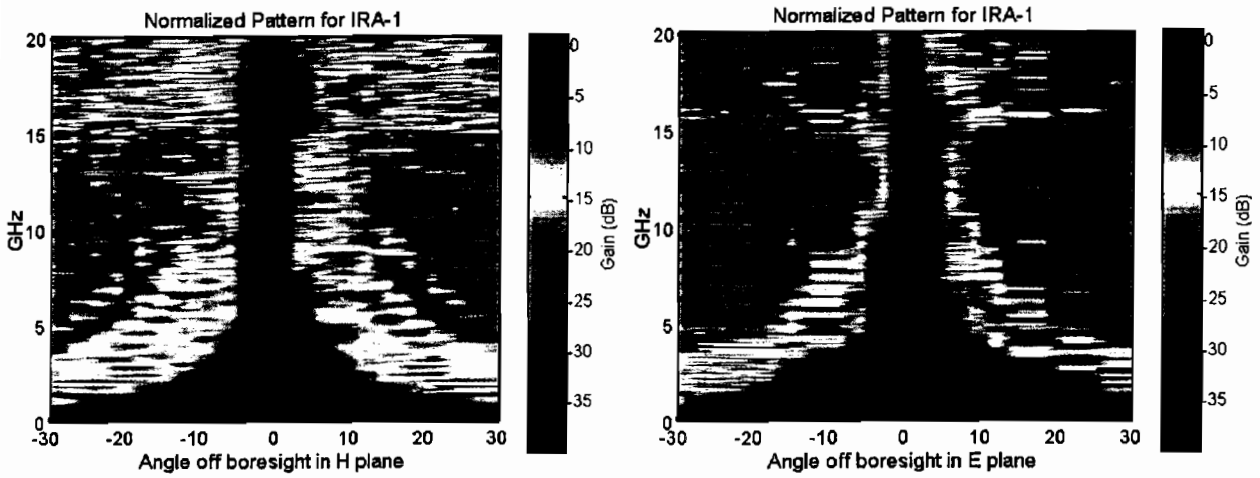

Figure 2.6. Normalized antenna pattern for the IRA-1. Angle is in degrees.

III. IRA-2.

We provide here corrected and expanded data on the version of the IRA-2 that was developed in [3]. This version is based on [1], with the feed arms positioned at ±30° to vertical. Photographs of the IRA-2 are shown in Figure 3.1. The feed arms for the IRA-2 have an included angle of 23.2°. The load resistor configuration is the same as for the original IRA-1, with High-Voltage Resistors (HVRs). .

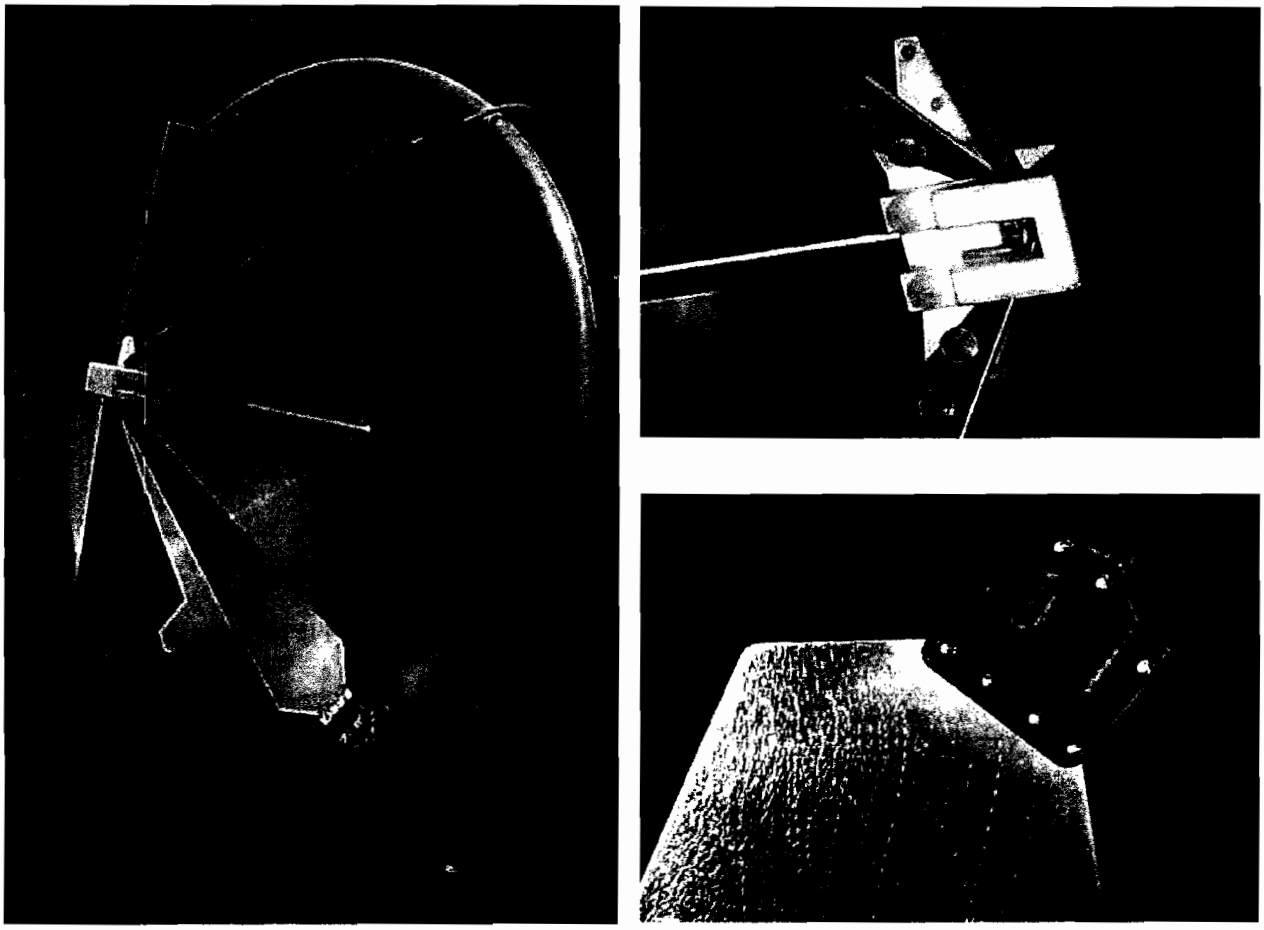

Figure 3.1. IRA-2 (feed arms at ±30°) with feed point and resistor details.

The TDR of the antenna is shown in Figure 3.2. As with the original IRA-1, we see a large dip in the impedance in the region of the resistors. Replacing the HVRs with a distributed load resistance would undoubtedly improve the TDR.

The normalized impulse response on boresight is shown in Figure 3.3. In the time domain, the FWHM of the impulse response is 34 ps and the aperture height is 133 mm. This is a 7% improvement over the IRA-1 presented above and 19% better than the original IRA-1. Since the IRA-2 is structurally closer to the original IRA-1, this improvement is even better than the expected 10%. This may be due in part to improvements in the feed point construction. The TDR

at the feed point is somewhat better than that of the IRA-1. The effective gain is shown in Figure 3.4. In Figure 3.5 we overlay the gains of the IRA-1 and IRA-2. The boresight gain of the IRA-2 is higher than that for the IRA-1 especially from 14 to 18 GHz. The crosspol rejection for the IRA-2 is considerably better than the IRA-1, except at frequencies below 6 GHz.

Figures 3.6 – 3.7 are the pattern plots in the H and E planes. The data from MRC is on the left and the data from FRI is on the right. The measurements from MRC were carried out in the frequency domain and those from FRI were carried out in the time domain. We only made measurements from 0° to +45°, so our data is replicated for the other side. This explains why the FRI data is perfectly symmetric, while the MRC data is not.

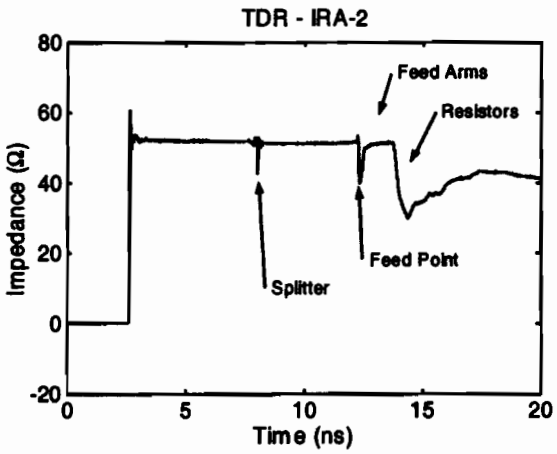

Figure 3.2. TDR of the IRA-2.

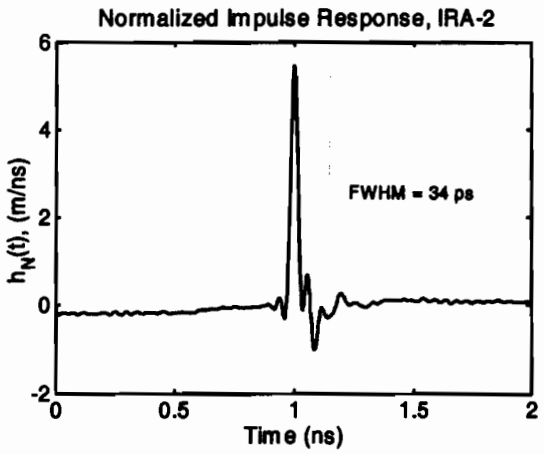

Figure 3.3. Normalized Impulse Response.

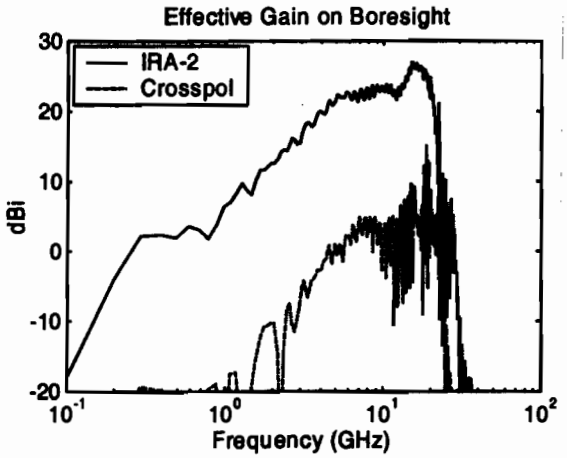

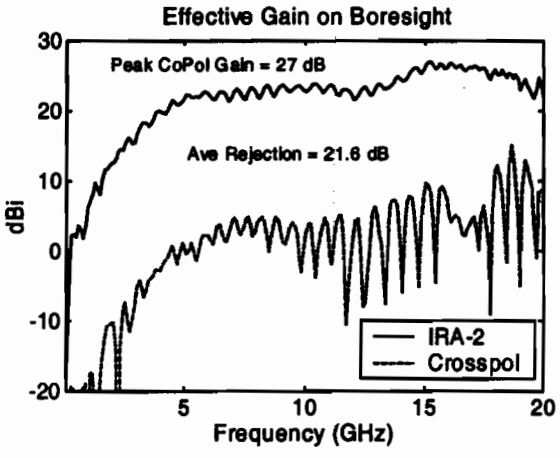

Figure 3.4. Effective gain of the IRA-2 on boresight including crosspol.

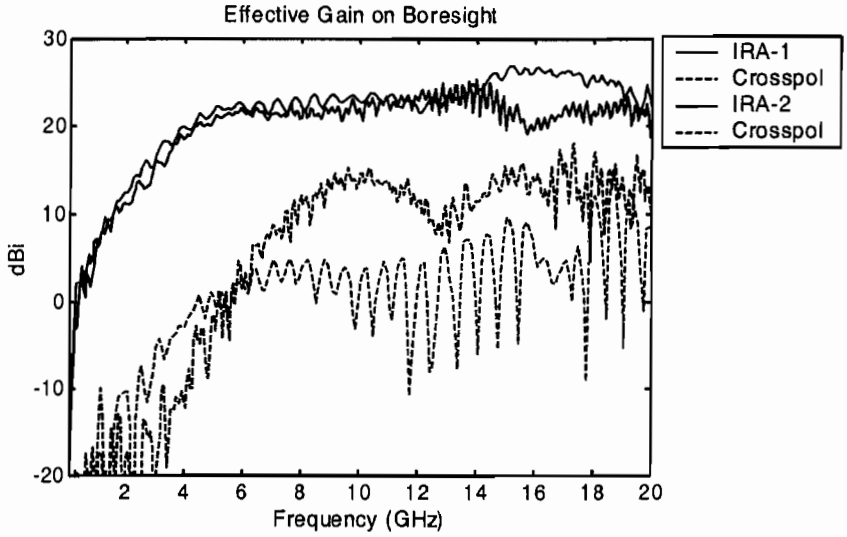

Figure 3.5. Comparison of IRA-1 and IRA-2 including crosspol.

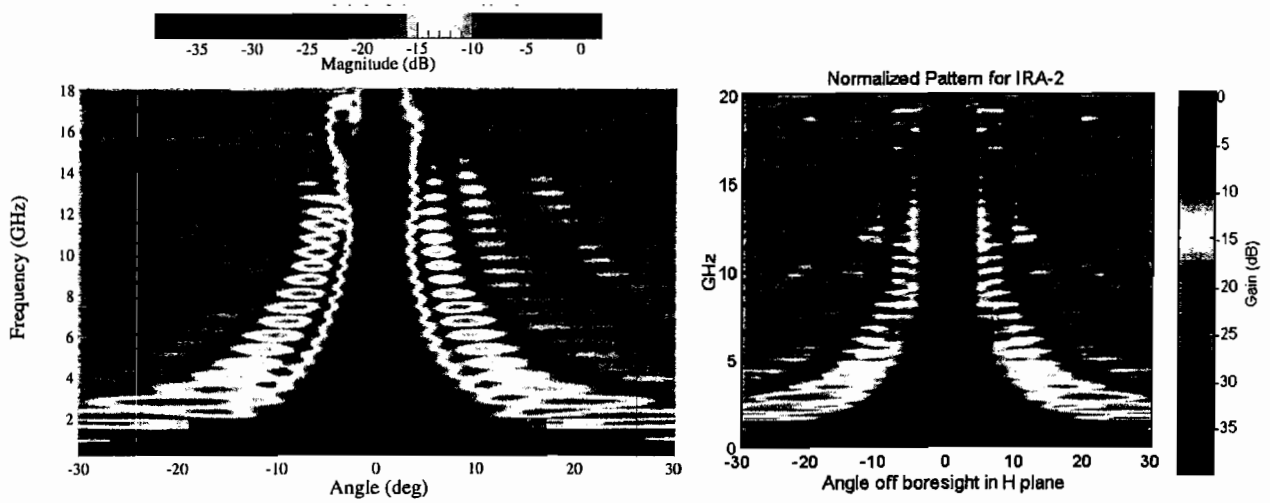

Figure 3.6. Pattern of the IRA-2 in the H plane, MRC left, FRI right. Angle is in degrees.

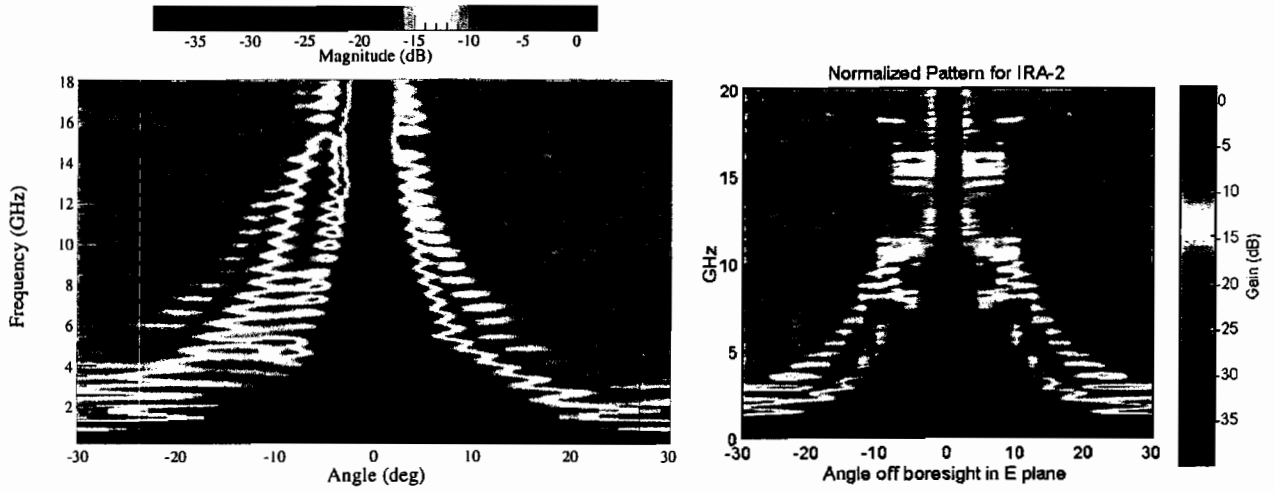

Figure 3.7. Pattern of the IRA-2 in the E plane, MRC left, FRI right. Angle is in degrees.

IV. IRA-3.

We next added a ground plane to the IRA, resulting in the IRA-3. We tried the ground plane to further reduce the crosspol, by shorting out the horizontal component of the E field, and to enhance the mechanical structure. We also tuned the resistors in the IRA-3, in order to minimize reflections. We also rebuilt the feed point with a new support structure.

The initial experiments performed on this version of the IRA were intended to improve the TDR in the area of the load resistance. For these experiments, we used the bottom half of the IRA-3, which normally has the feed cable along the axis of rotation of the antenna. For the case with a ground plane, this cable is attached to the surface of the ground plane, as shown in Figure 4.1. Also shown in this figure is the feed arm support ring. This ring is made of UHMW, which has a relative dielectric constant of 2.3. Using only half of the IRA made it possible to speed up the experimental process, since we only had to construct two load resistor configurations for each test, instead of four. While tuning the resistors, we found that the standard ground plane was much too small, so we used a larger ground plane for many of the experiments.

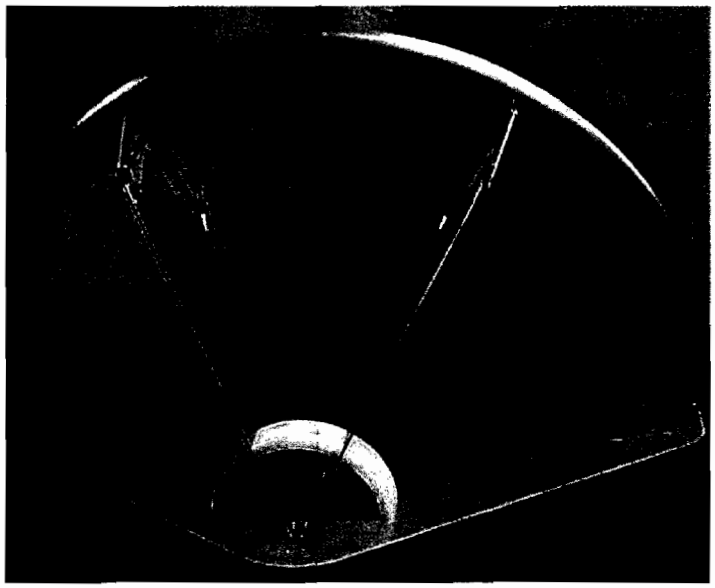

Figure 4.1. Half IRA-3 with ground plane and feed from the rear.

In the first experiments, we used five 1-kΩ resistors at the end of each arm, in place of the two 400-ohm HVRs used in the past. It was hoped that distributing the resistance over the end of the feed arm would improve the TDR, as it did for the IRA-1. Although several configurations were tested, we found that a distributed load was not optimal for the IRA-3 with feed arms positioned at ±30°. All of the configurations tested with a distributed load produced a large dip in the impedance in the region of the load resistors.

The dip in impedance at the load resistors is due in part to the electric field incident on the center of the parabolic reflector at time F/c where c is the speed of light in free space. The

reflected field has a ramp-function time dependence, and it appears in the TDR as a negative dip at time $2F/c$ [10]. We conducted a series of experiments to determine the effects of various load resistor, feed arm, and feed point configurations. Noting that the large dip in the TDR is a capacitive effect, we attempted to add some inductance at the right place to counteract it. The inductance was added by using small hand-made coils of various sizes and shapes, with 2 to 16 turns. We found 10 turns worked particularly well. The coils were wound in a figure 8 pattern to reduce the magnetic moment of the coils, thereby reducing emissions from the coil [12]. We tried various feed arm lengths, as well as many different resistor and coil configurations.

In Figure 4.2, we show a detail of the load configuration and the associated TDR which gave the best results. This TDR was taken on a complete 4 arm IRA. Note that a reverse taper at the end of the feed arm begins just before the 9-inch point, which is one focal length from the feed point. So the inductance is seen at the same time that the wave strikes the center of the reflector. There are several important things to notice about the TDR of this antenna. First, the TDR at the feed point is reasonably typical of what we are able to achieve on the IRAs. Second, the impedance of the feed arms is reasonably flat and close to 50 ohms, except near the plastic support ring.

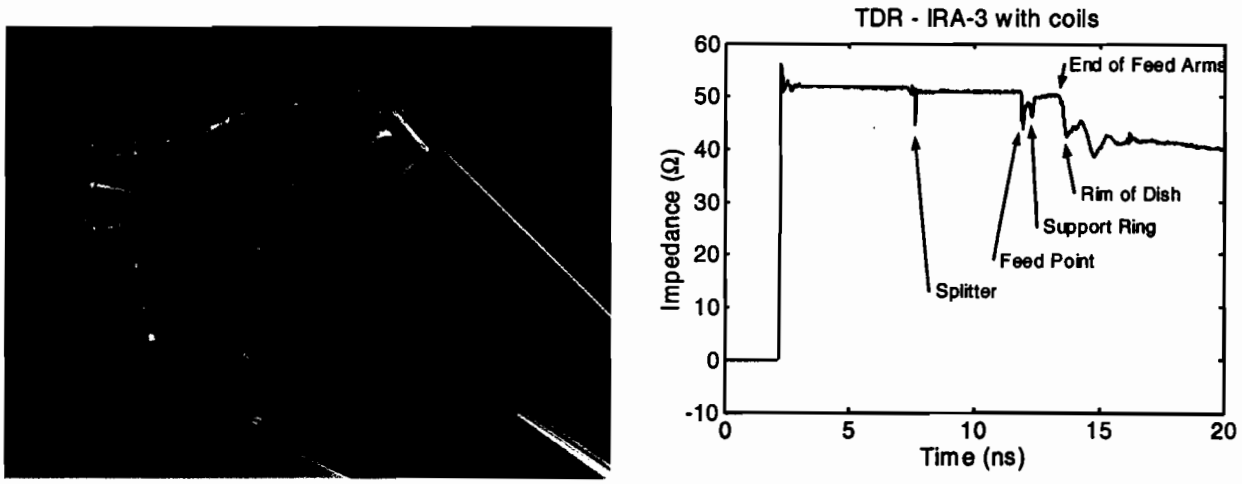

Figure 4.2. Two strings with a 10 turn figure 8 coil, a 180 Ω resistor, and a 220 Ω resistor.

Next, we moved the lower feed to the front of the feed point, as shown in Figure 4.3 (shown here upside down). Up to this point, the lower feed cable has always approached the feed point from the rear (up through the center) as shown in Figure 4.1. This is also true of the IRA-1 and IRA-2, since one feed cable passes through the center support tube on the axis of rotation. The feed configuration on the other side of the ground plane was not changed. Moving the feed to the front launches the wave toward the reflector, which improves the TDR at the feed point and the overall antenna gain. In doing this, the crosspol rejection was also somewhat improved. We also tried "unzipping" the coax cable at the feed point, but we found this did little to improve the TDR. Since a zipper connection is time-consuming to build, we did not pursue that design further.

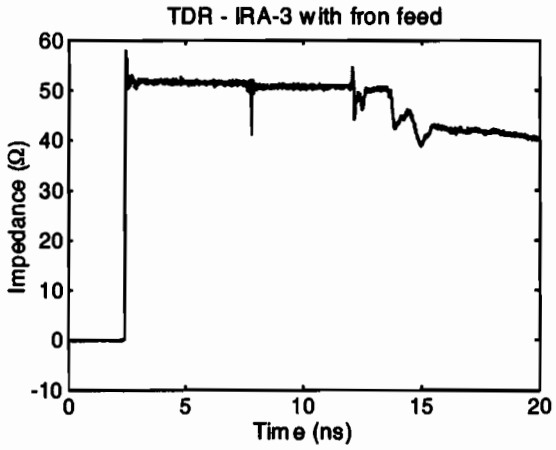

Figure 4.3. IRA-3 with the feed from the front.

In the above configuration, the load was made up of two parallel strings, each with a 10 turn figure 8 coil, a 180-ohm resistor, and a 220-ohm resistor. The resistors were carbon composition types, which have almost no inductance. Since the above configuration worked well, it appears that some distributed inductance may be helpful. For this reason, we removed the coils and replaced the carbon composition resistors with metal film resistors, which have a small inductance. Figure 4.4 shows the load configuration and the associated TDR for this modification. The TDR for this case is almost identical to the one in Figure 4.2. Therefore, we stayed with this load configuration since it is considerably easier to build, and stronger. Furthermore, the metal film resistors are more readily available than the carbon composition type.

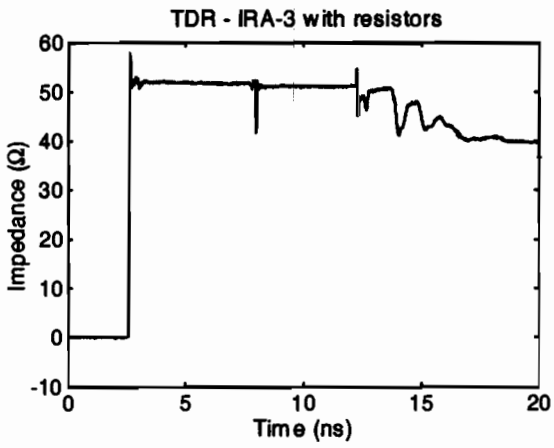

Figure 4.4. Four 200 Ω metal film resistors in series/parallel.

Next, we investigated covering the resistors with microwave absorber foam, in order to reduce spurious radiation that could increase sidelobes. First, the load regions were first wrapped with plastic to insulate the load from the slightly conductive foam. Next, the area was covered with 2 layers of 1/8-inch thick absorber foam. We then took a TDR of the configuration, and we observed a drastic drop in impedance at the resistors, due to the presence of the foam. We found

this even though the foam was not in contact with the resistors. Due to the very poor TDR, this configuration was abandoned.

The next modification to the IRA-3 was the addition of dummy cables to improve the symmetry of the antenna near the feed point. C. E. Baum has shown in [7] that the crosspol coupling in an IRA can be greatly reduced by maintaining the symmetry about horizontal and/or vertical planes of symmetry. In this case, we chose to maintain symmetry about the vertical plane. Thus, we place a short section of cable between the feed point and UHMW support ring, as shown in Figure 4.5 (left). On the bottom side of the ground plane we added another dummy cable, as shown in Figure 4.5 (right). When we reconnected the feed arms to the center conductor of the feed coax, we were not able to get the connection as close as desired. Therefore, the TDR at the feed point, shown in Figure 4.6, is not quite as good as it was in Figure 4.3. Very close connections at the feed point improve the gain at high frequencies.

In spite of the long connection at the feed point, the overall characteristics of this antenna are quite good. The normalized impulse response is given in Figure 4.7. The FWHM of the impulse response is 35.5 ps and the aperture height is 139 mm. The effective gain is shown in Figure 4.8. The peak effective gain of the antenna is 26.5 dBi. The average crosspol rejection is 24 dB. In Figure 4.8 we include the gain of the IRA-2 for easy comparison. The normalized antenna patterns are shown in Figures 4.9 and 4.10.

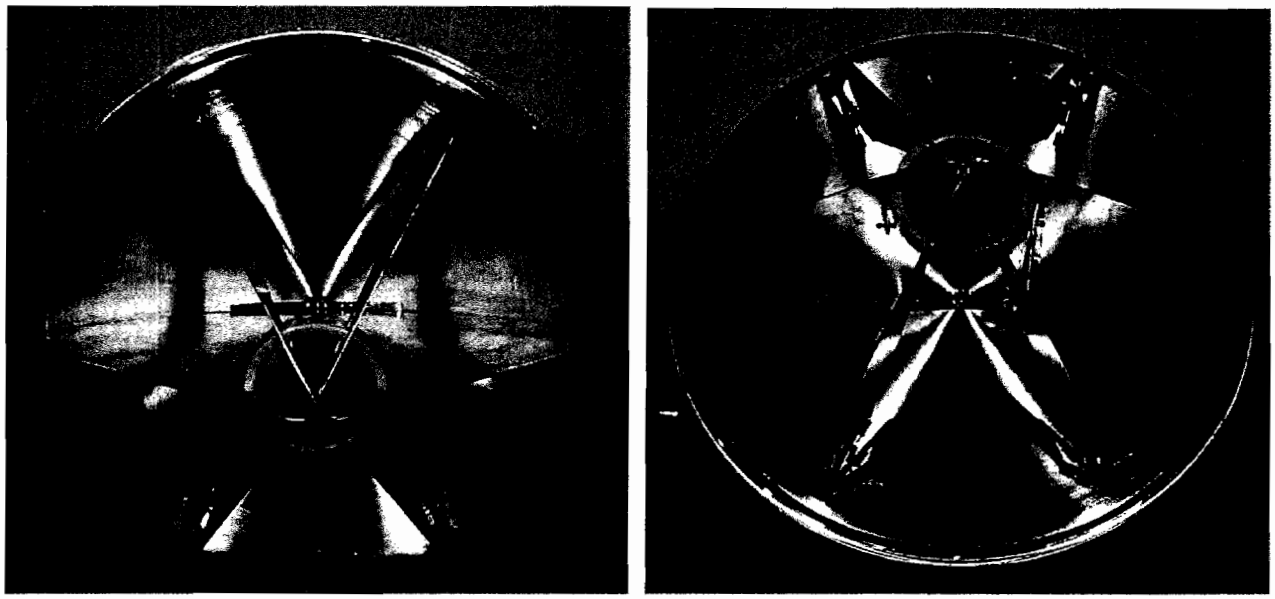

Figure 4.5 IRA-3 with dummy cables added for symmetry.

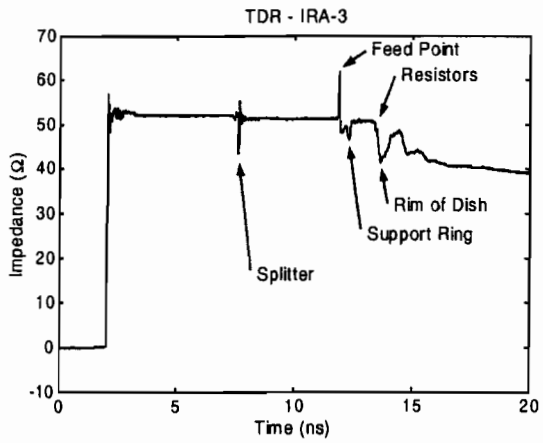

Figure 4.6. TDR with dummy cables.

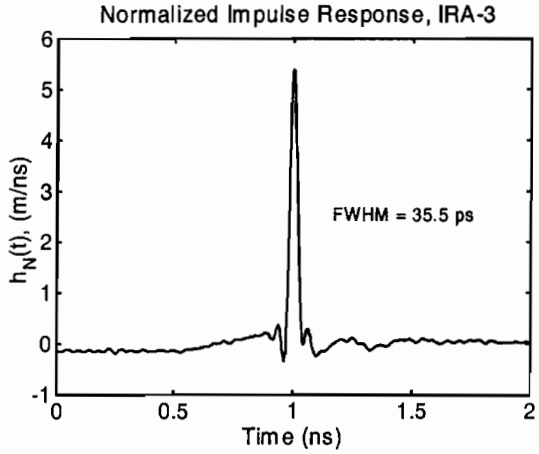

Figure 4.7. Normalized Impulse Response.

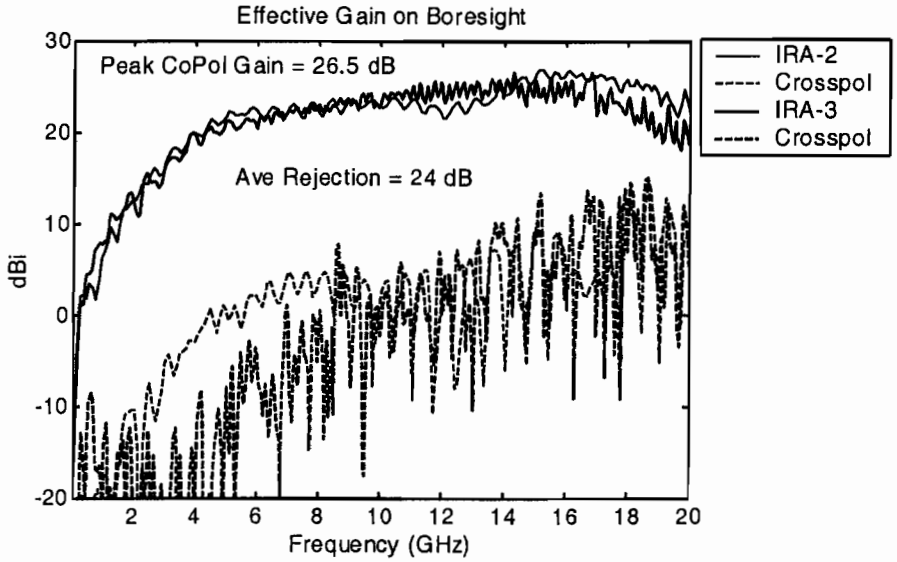

Figure 4.8. Effective Gain on Boresight of the IRA-3 with the IRA-2 included for comparison.

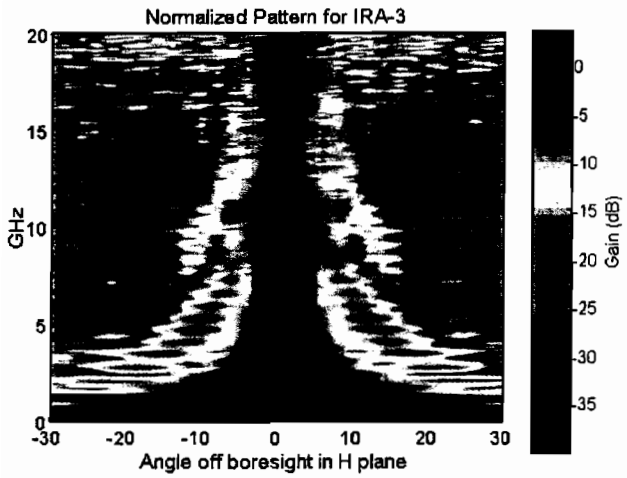

Figure 4.9. Pattern in the H plane. Angle is in degrees.

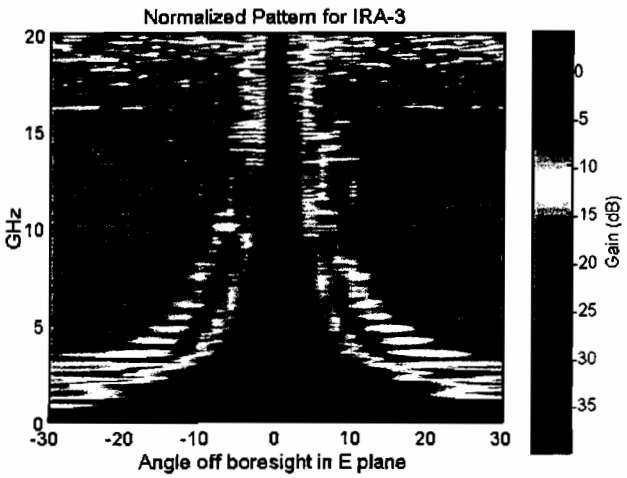

Figure 4.10. Pattern in the E plane. Angle is in degrees.

Next, we consider a radome that was attached to the IRA-3 by MRC Dayton. This was attached to the original (prototype) IRA-3 (IRA-3-0). The radome is made from two glass/epoxy skins with a Nomex core. The IRA-3 with the radome is shown in Figure 4.11. The radome protects the feed elements of the IRA, and it may be required if the antenna is mounted to the outside skin of an aircraft.

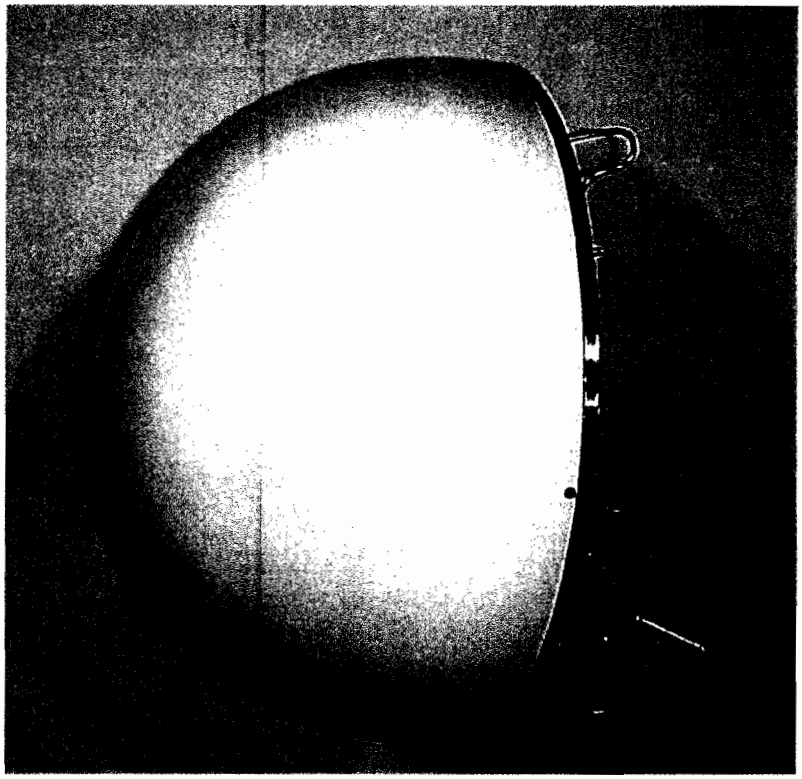

Figure 4.11. IRA-3 with radome manufactured by MRC.

We now consider the performance of the antenna with the radome attached. The radome only slightly changes the TDR as seen in Figure 4.12. In Figure 4.13 we see that the peak of the normalized impulse response is reduced by about 10% from that shown in Figure 4.6 before the radome was installed. In Figure 14 we plot the gain of the IRA-3 both with and without the radome. Below about 10 GHz the gains are almost identical. The radome reduces the peak gain slightly, but does not appreciably change the aperture height. We provide pattern plots in Figures 4.15 - 4.16 from both FRI and MRC, generated by two different experimental methods (time domain versus frequency domain). The pattern plots using the two methods are in very good agreement.

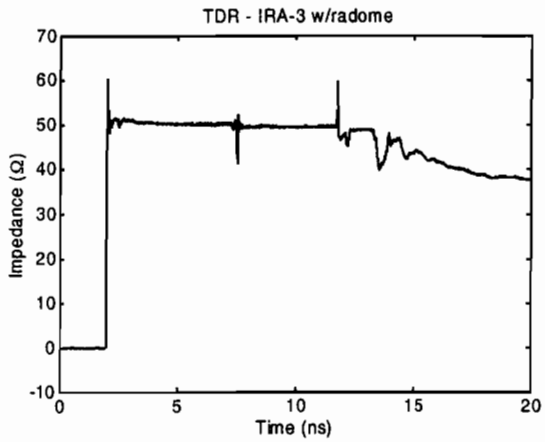

Figure 4.12. TDR of IRA-3 with radome.

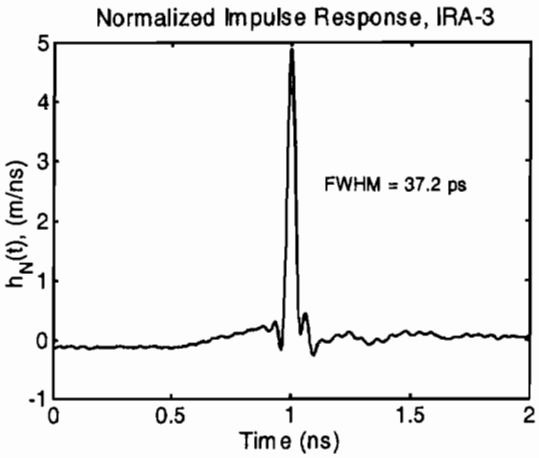

Figure 4.13. Normalized Impulse Response.

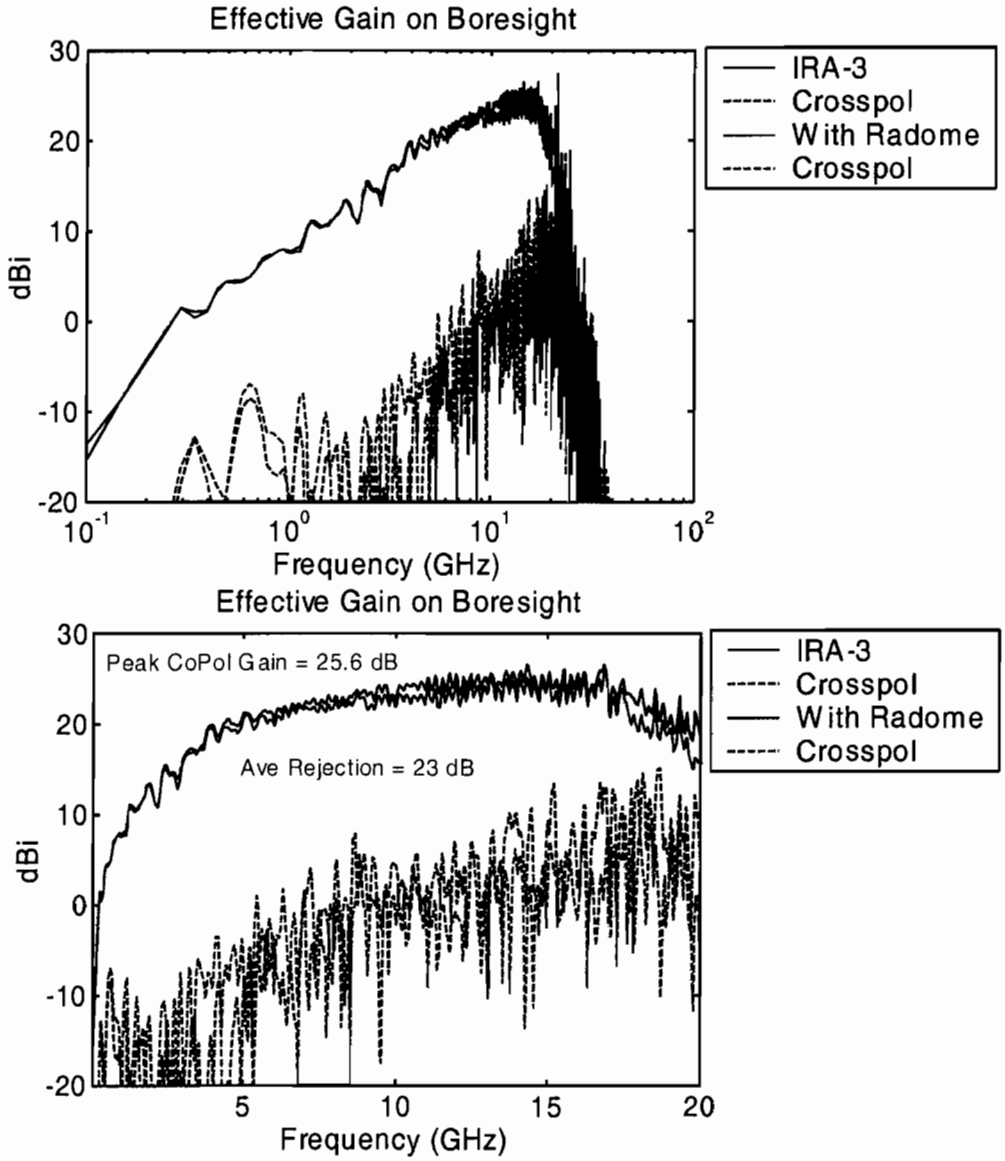

Figure 4.14. Effective gain of the IRA-3 with and without the radome.

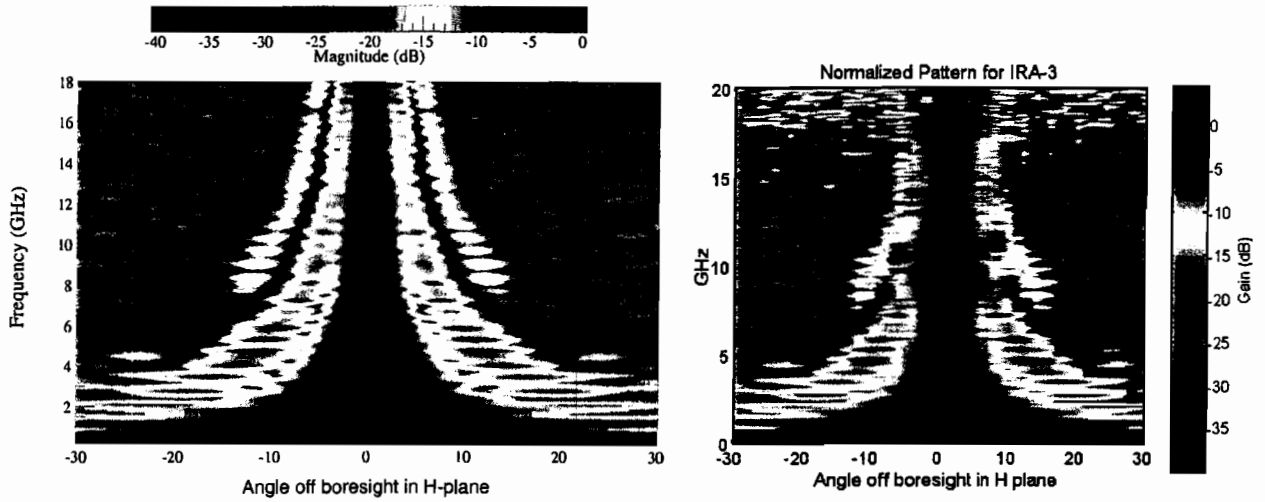

Figure 4.15. Pattern of the IRA-3 in H plane, MRC left, FRI right. Angle is in degrees.

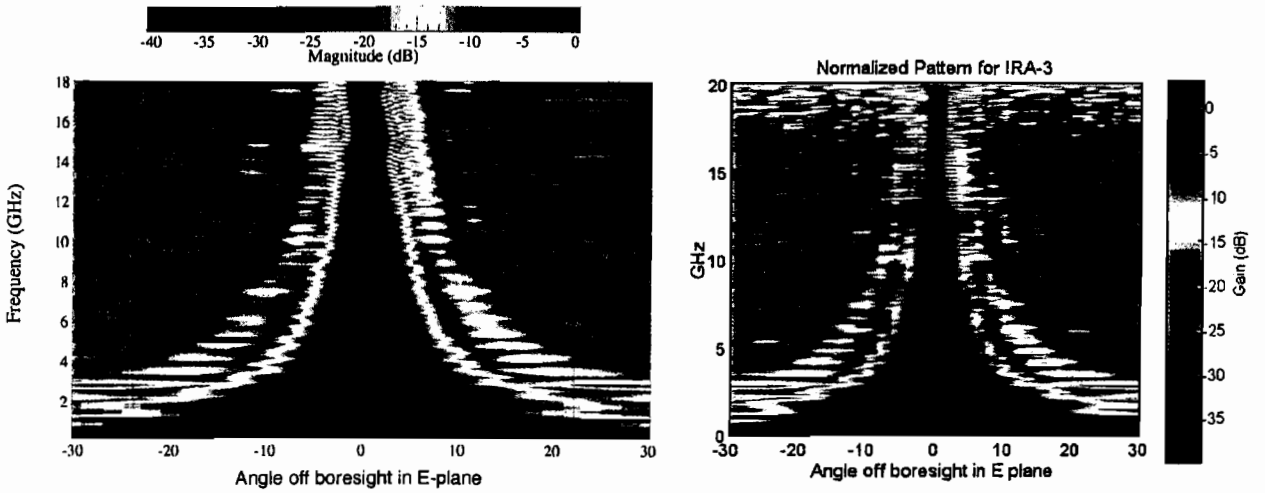

Figure 4.16. Pattern of the IRA-3 in the E plane, MRC left, FRI right. Angle is in degrees.

The last modification to the IRA-3 was the addition of absorber foam around the rim of the reflector dish. The foam was intended to reduce the fields near the edge of the reflector, and to reduce the E field in areas where the polarity is reversed. The IRA-3 with the foam in place is shown in Figure 4.17. The foam was 1.125 inches thick, and according to the manufacturer, this foam is designed for use at frequencies above 2.5 GHz. The foam extends over the portion of the reflector between the feed arms where the E field has the incorrect polarity. The radome was replaced before making the measurements reported below.

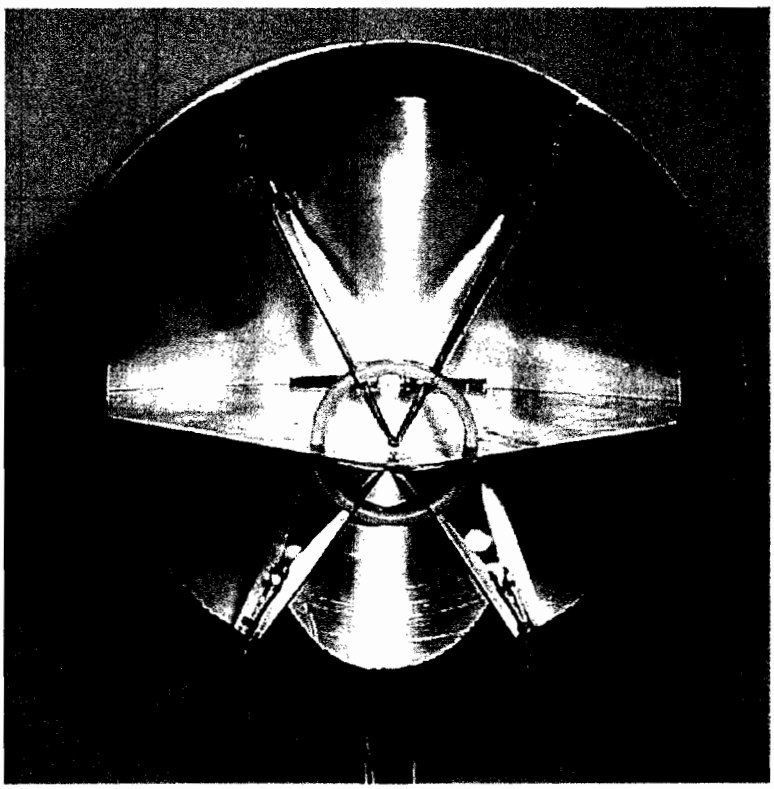

Figure 4.17. IRA-3 with absorber foam.

We now consider the results with the foam. The foam changes the late time TDR a little, as shown in Figure 4.18. We see from Figure 4.19 that the foam reduces the peak of the impulse response. The aperture height for this IRA is 112 mm, which is somewhat lower than expected. In Figure 4.20 we see that the peak gain is reduced by about 1 dB and the average crosspol rejection is reduced by nearly 3 dB, when compared to Figure 4.14. These compromises in performance might be acceptable if the sidelobes were reduced. Unfortunately, little change can be seen in the sidelobes as shown in Figures 4.21 – 4.22.

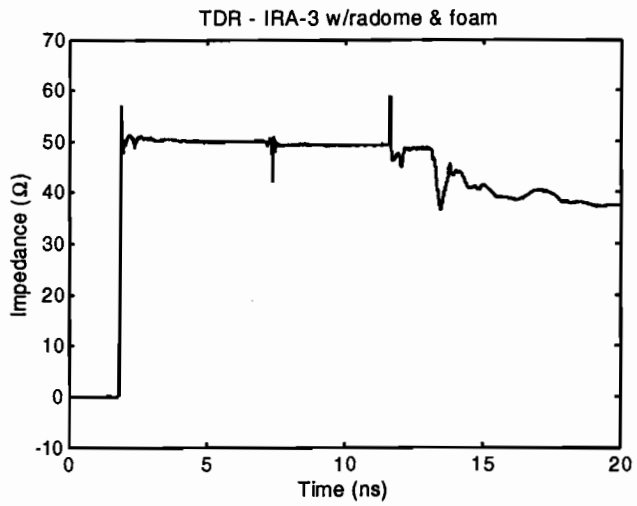

Figure 4.18. TDR with radome and foam.

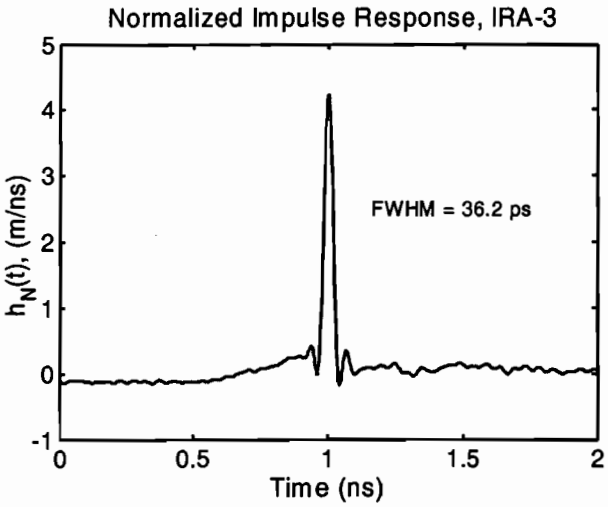

Figure 4.19. Normalized Impulse Response.

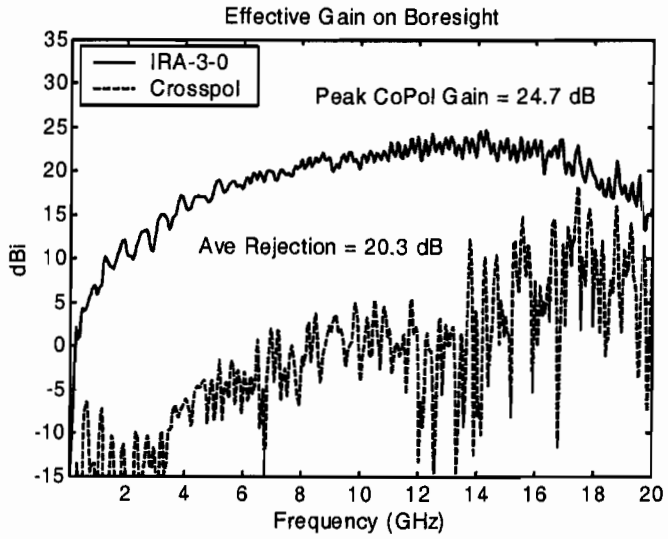

Figure 4.20. Effective gain of the IRA-3 with radome and absorber foam.

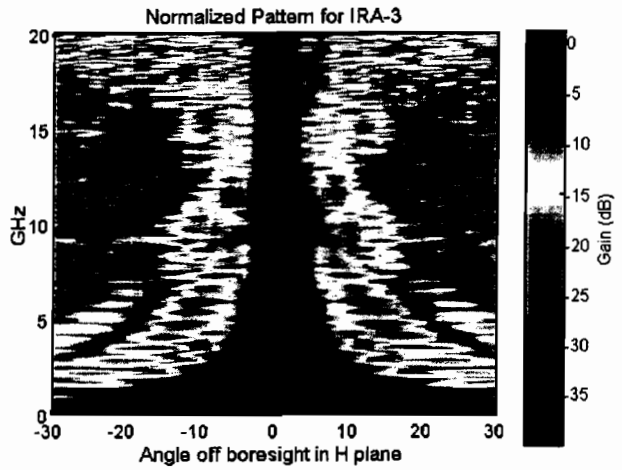

Figure 4.21. Pattern in the H plane. Angle is in degrees.

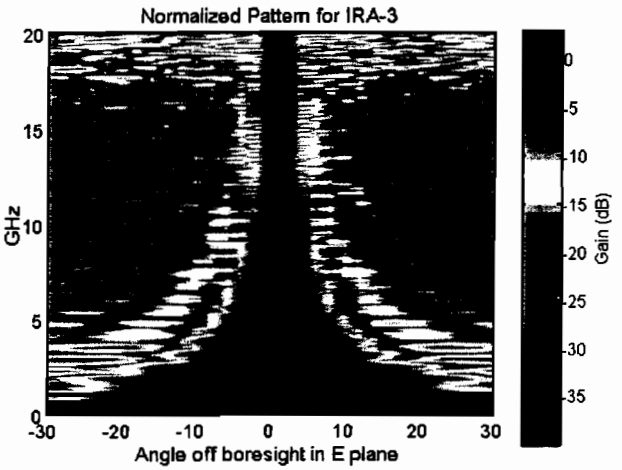

Figure 4.22. Pattern in the E plane. Angle is in degrees.

As a result of our studies on the IRA-3, we have learned a number of things. We have found that adding a ground plane reduces crosspol and makes the antenna more sturdy. We found a configuration of metal-film resistors that reduces reflections at the ends of the feed arms. We found that feeding the antenna from the front provides lower TDR losses at the feed point. We found that dummy cables do not reduce crosspol appreciably. We found that adding foam does not reduce sidelobes. Finally, we found that adding a radome seems to affect performance very little. We next turn our attention to the IRA-4.

V. IRA-4.

Finally, we repositioned the feed arms so their outer edge is aligned with the outer edge of the reflector, resulting in the IRA-4. We did this to reduce the sidelobes by concentrating the field closer to the center of the reflector. Modifying the feed arm location in this way required recalculating the included angle of the feed arms to match the required 200-ohm impedance. The included angle of the feed arms for the IRA-4 is 20°.

A second modification we made in the IRA-4 was the development of an improved splitter. This device has a 50-ohm SMA connection that splits into two 100-ohm 0.141" semi-rigid lines. The new splitter has an extremely flat TDR, as shown in Figure 5.1. We have overlaid the TDR of the splitter we used previously, manufactured by Prodyn Technologies, so one can see the improved impedance match.

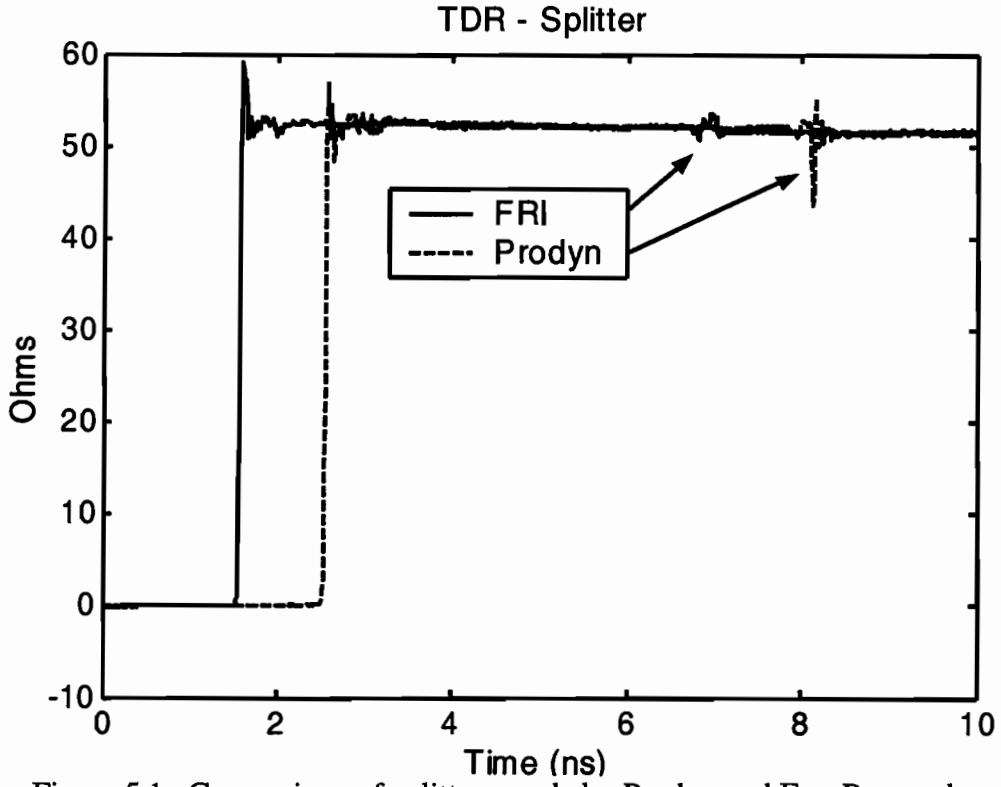

Figure 5.1. Comparison of splitters made by Prodyn and Farr Research.

Figure 5.2 is a photograph of the IRA-4. In this early data, this antenna does not have the dummy cables for improved symmetry. These cables will be added later in this report, and new results will be provided. The TDR is shown in Figure 5.3. The drop in impedance at the load resistors suggests that there is room for improvement in their design. This is not surprising, because the resistors were not tuned to the degree they were in then IRA-3. In Figure 5.4 we show the normalized impulse response. Based simply on the area between the feed arms where the E field has the wrong polarity, we expected the gain of the IRA-4 to be about 2 dB less than the gain of the IRA-3, and this is approximately what we observe in Figure 5.5. The aperture height is 126 mm, which is about the same as the IRA-3 before the dummy cables were added.

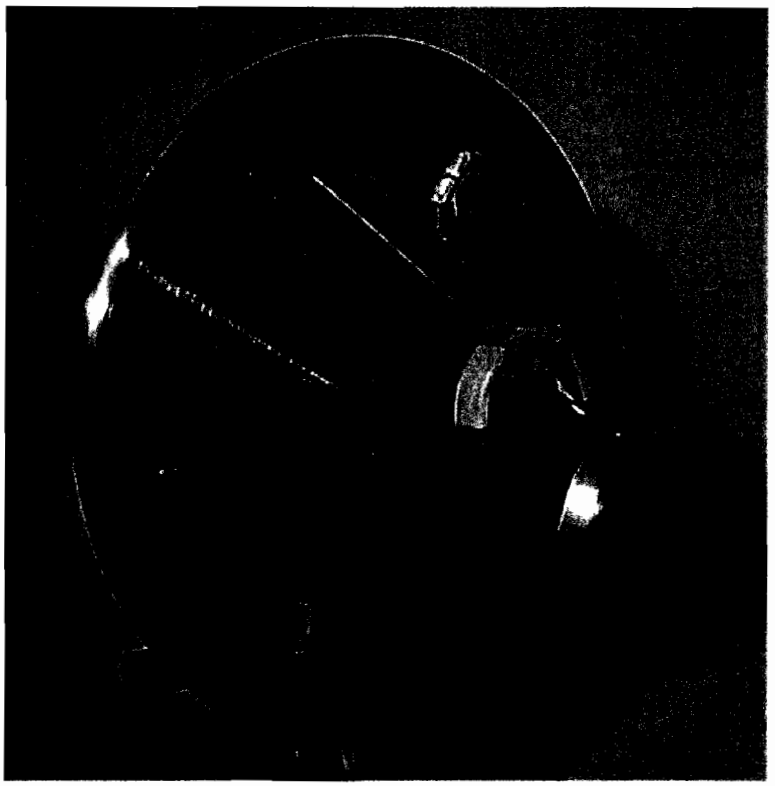

Figure 5.2. IRA-4.

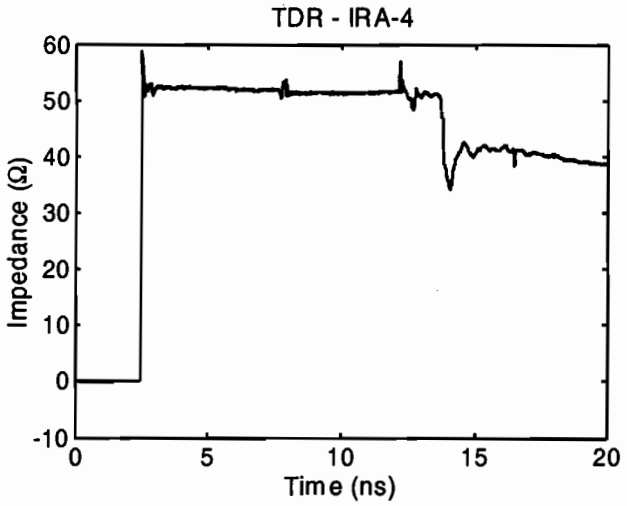

Figure5.3. TDR of IRA-4.

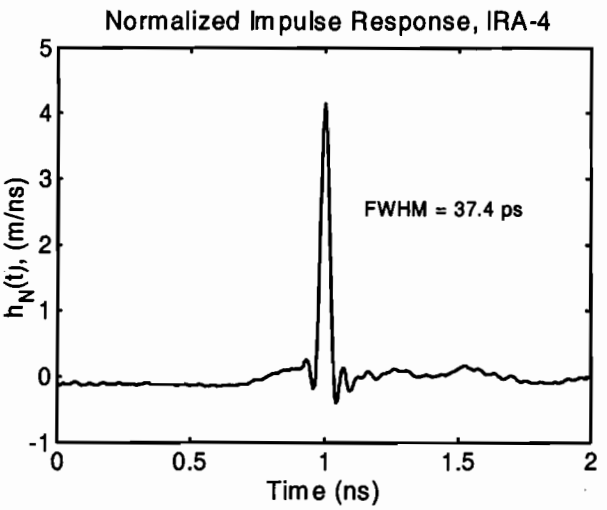

Figure 5.4. Normalized Impulse Response.

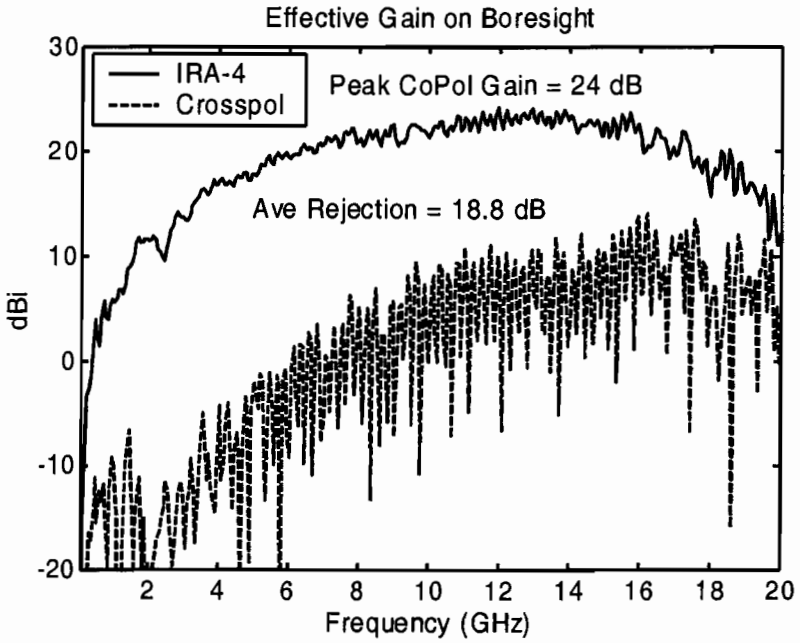

Figure 5.5. Effective gain of the IRA-4.

The patterns in the H and E planes are shown in Figures 5.6 and 5.7. Recall that the goal of this design was to reduce the sidelobes. However, in the H plane the sidelobes are quite pronounced, so moving the feed arms closer to the center does not seem to help.

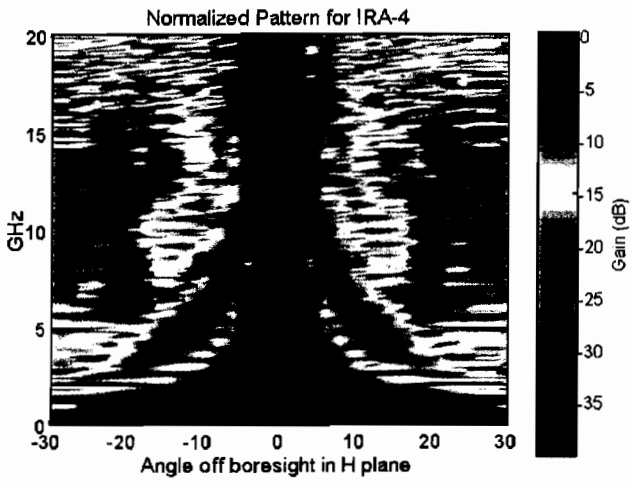

Figure 5.6. Pattern in the H plane. Angle is in degrees.

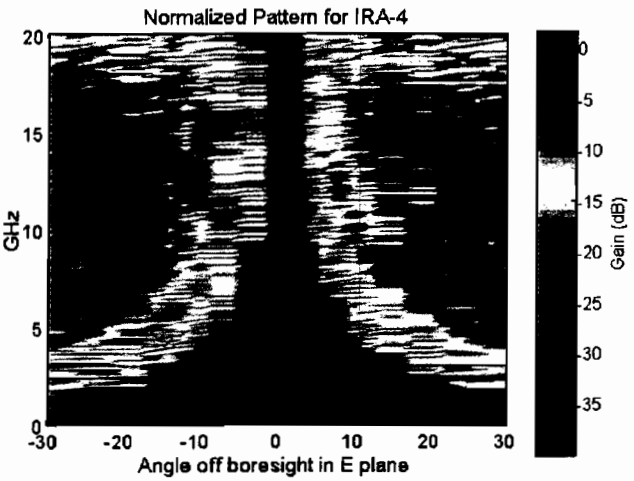

Figure 5.7. Pattern in the E plane. Angle is in degrees.

Next, we added dummy cables to the IRA-4. The ground plane on the IRA-4 is extended slightly, to provide more room for the lower feed cable to approach the feed point from the front. The locations of the dummy cables are shown in Figure 5.8. Note that the cables are extended considerably further from the feed point, and that the cables are not right on the front edge of the ground plane as they were on the IRA-3.

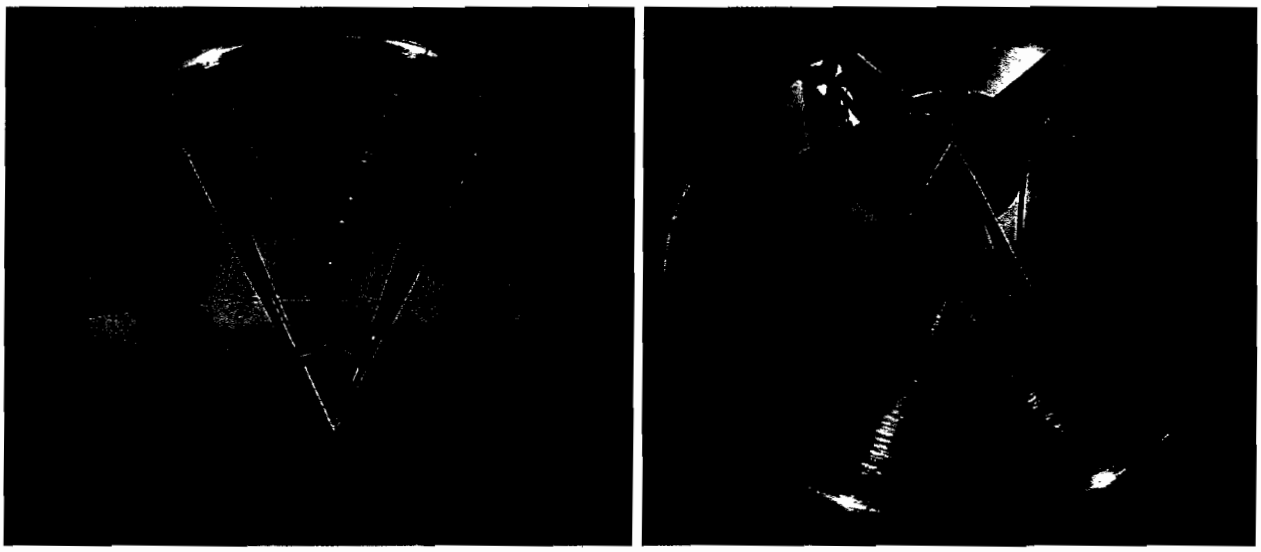

Figure 5.8. IRA-4 with symmetry cables installed.

We now provide the results of adding the dummy cables to the IRA-4. The TDR of the antenna is shown in Figure 5.9. The peak of the normalized impulse response increased slightly as shown in Figure 5.10. The aperture height is 118 mm, which is a 7% improvement. In Figure 5.11 we see that the peak effective gain and the average cross polarization rejection are improved by approximately 1 dB. We expected that adding the dummy cables would improve the crosspol rejection considerably more than 1 dB, however, we have seen little effect from the dummy cables.

There are a couple of items that may be worth noting concerning the measurements in the crosspol configuration. First, the dynamic range of the outdoor time domain antenna range is estimated to be about 30dB, so some of the crosspol measurements may be close to the noise level our system. Second, when making crosspol measurements, we normally rotate the antenna under test (AUT) such that the dominate E field is horizontal. A television transmitter is now located within 10 miles of the test range at about 60° off boresight. Since TV signals are horizontally polarized this could be a source of noise. We have noticed that the noise level with the AUT in the horizontal position is about twice what it is in the vertical position. This reduces the dynamic range by about 6 dB.

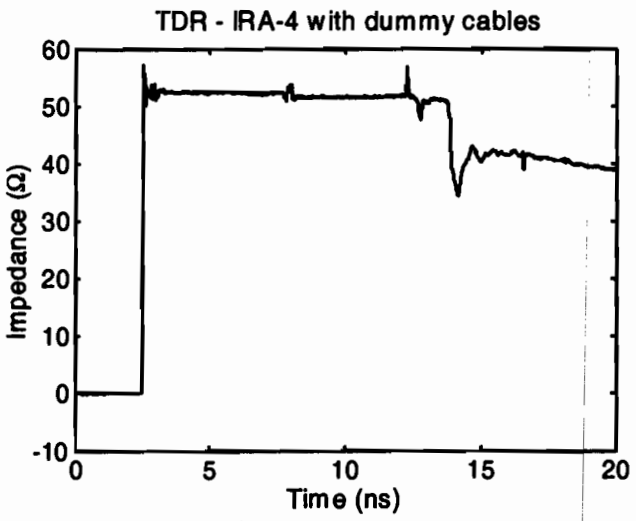

Figure 5.9. TDR of IRA-4.

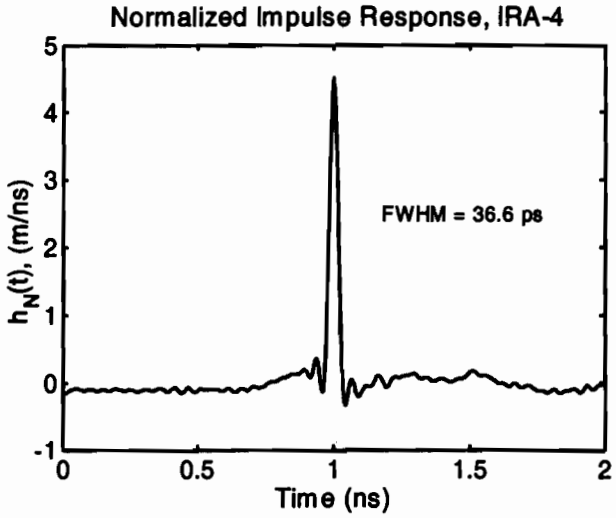

Figure 5.10. Normalized Impulse Response.

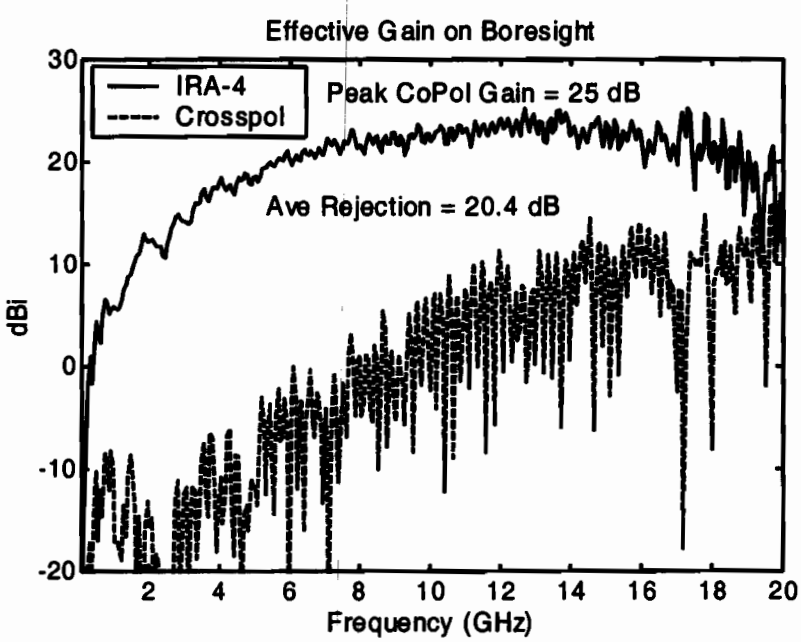

Figure 5.11. Effective gain of the IRA-4 with symmetry cables.

The antenna patterns are provided in Figures 5.12 - 5.13. The sidelobes at about 5 GHz in the H plane are about the same as before.

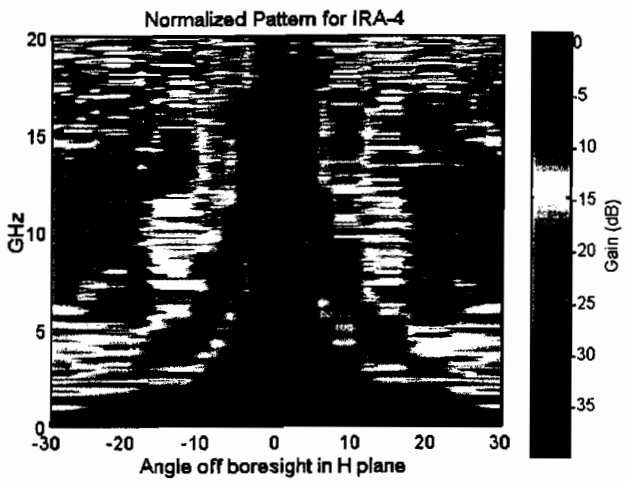

Figure 5.12. Pattern in the H plane. Angle is in degrees.

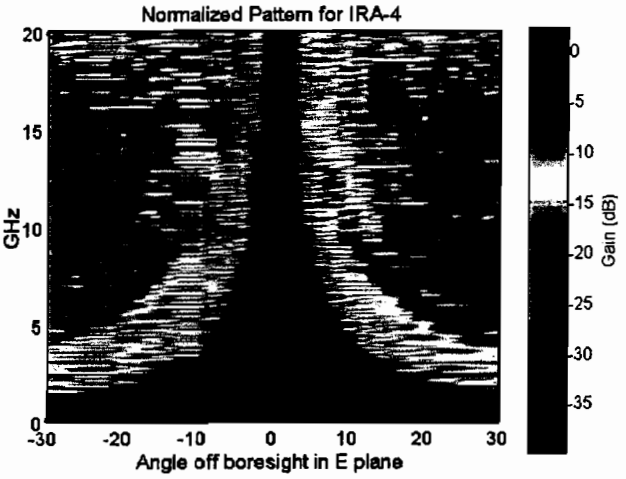

Figure 5.13. Pattern in the E plane. Angle is in degrees.

For a final comparison, we add absorber foam around the rim of the reflector dish on the IRA-4. The ¾-inch thick foam, shown in Figure 5.14, is designed for use at frequencies above 3.5 GHz. Between the feed arms we extended the foam to cover the area where the electric field has the incorrect polarity. This is a larger area than that of the IRA-3. Covering this area should improve the gain of the antenna.

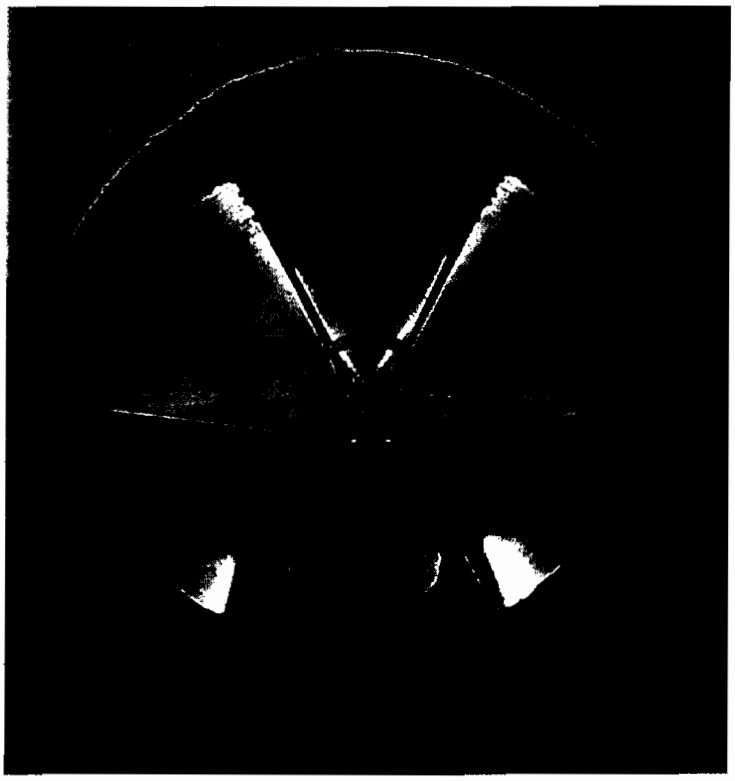

Figure 5.14. IRA-4 with absorber foam around rim.

We now consider the results obtained with the IRA-4 with dummy cables and foam. First, the TDR is shown in Figure 5.15, and it is largely unaffected by the addition of the dummy cables and absorber foam, as seen in Figures 5.3, 5.9, and 5.15. Next, the normalized impulse response is shown in Figure 5.16, which has changed little from the last iteration without the foam. Next, the effective gain and crosspol gain are shown in Figure 5.17, and they are compared to the IRA-3 with the radome and absorber foam. While the gain of the IRA-4 is about the same, the crosspol has increased. Finally, the antenna pattern is shown in Figures 5.18 - 5.19, where we see that there is no real reduction in the sidelobes with the use of the absorber foam.

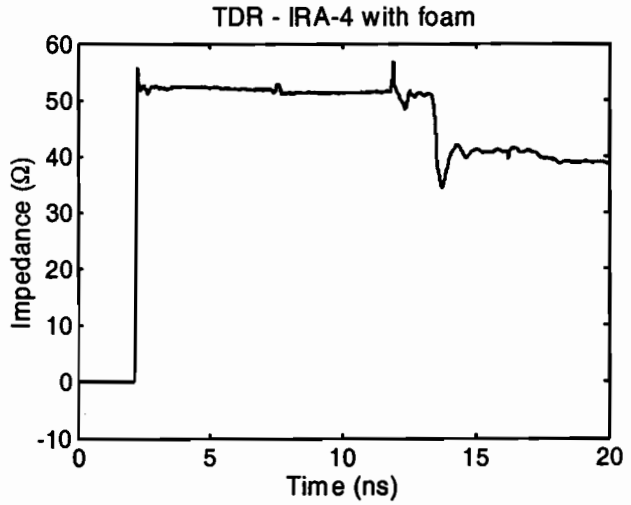

Figure 5.15. TDR with dummy cables & foam.

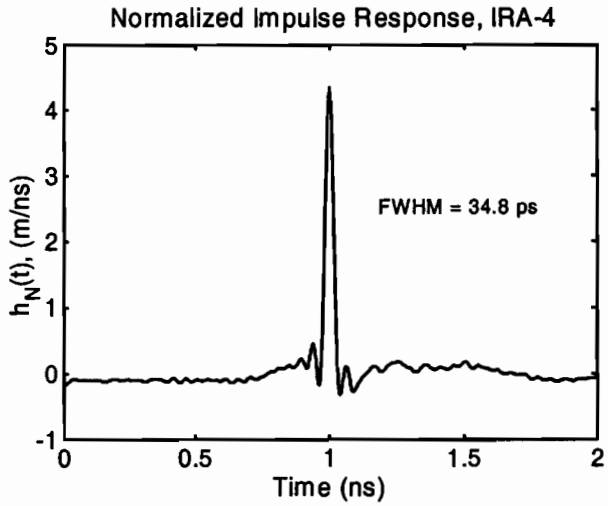

Figure 5.16. Normalized Impulse Response.

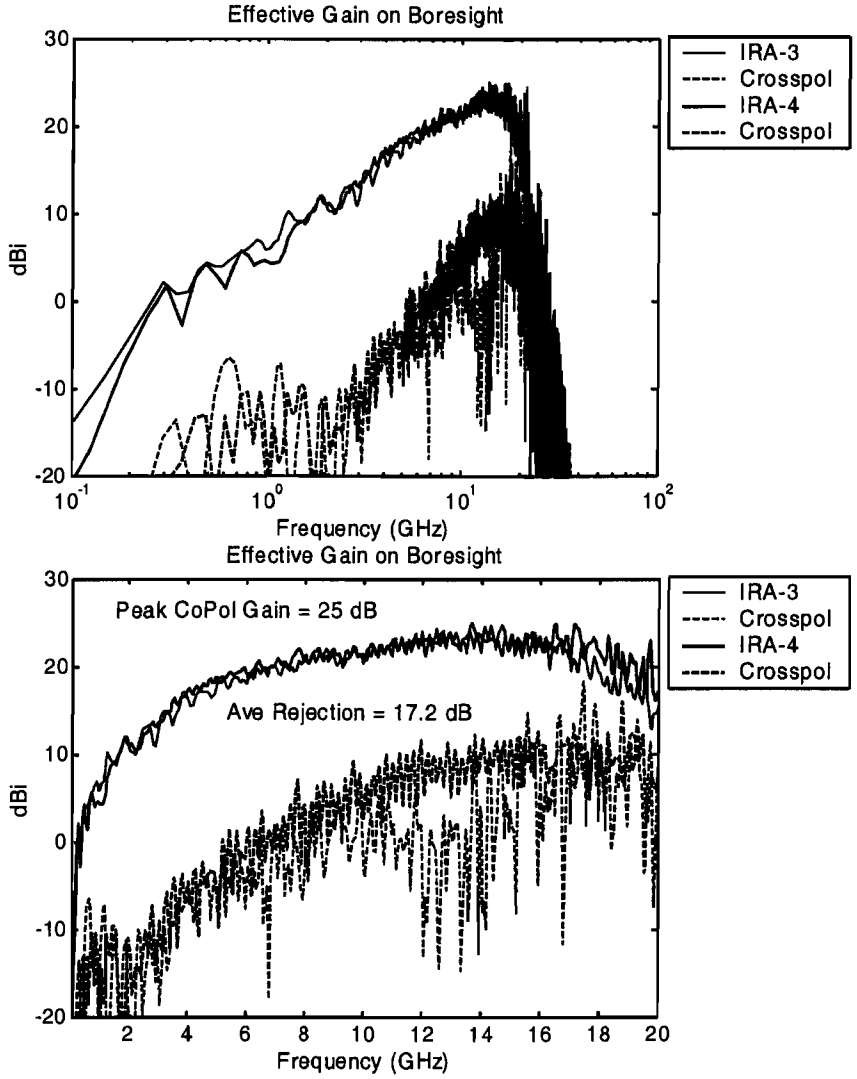

Figure 5.17. Comparison of the effective gain of the IRA-4 and the IRA-3 (from Figure 4.20)

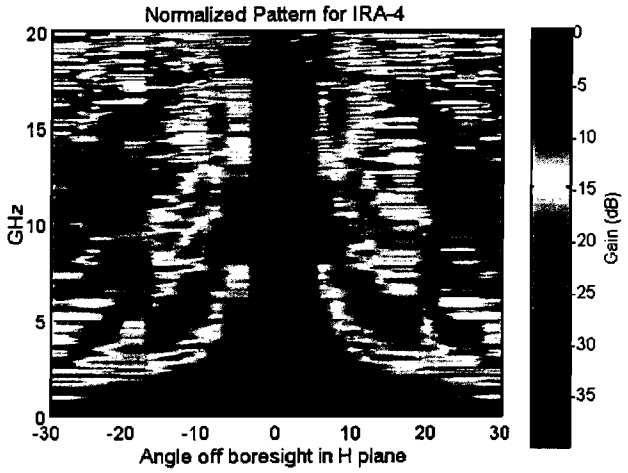

Figure 5.18. Pattern in the H plane. Angle is in degrees.

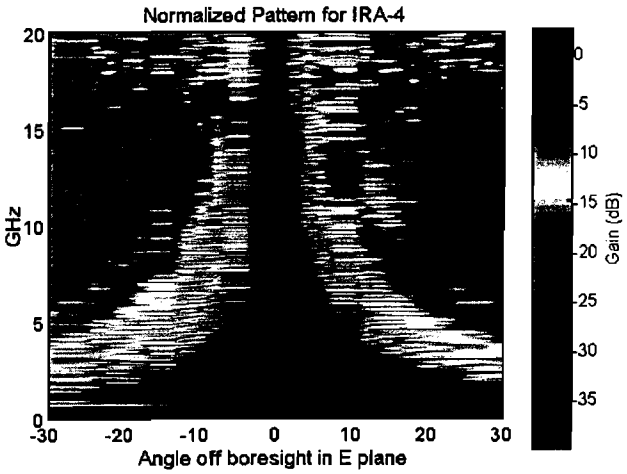

Figure 5.19. Pattern in the E plane. Angle is in degrees.

VI. Discussion.

In Table 1 we summarize the results of the antennas described in this paper, and on a number of additional minor variations. The table includes the major parameters of interest in the optimization of the IRA. The peak gain column includes not only the peak gain in dBi, but also the frequency at which it occurs. The minimum cross polarization rejection is included as well, but it may be of little value since it is frequently zero or negative, due to the high noise level in the crosspol signal. In cases where the value is negative it is set to zero. In the Load Configuration column of the table, the word "Inductive" refers to 2 strings of metal film resistors in parallel. The strings may have from 1 to 3 resistors. We had wanted to include sidelobe level, but this is difficult to quantify as a function of frequency, so it is not included.

From Table 1, we can observe that a number of important improvements have been made to the IRA. Moving the feed arms from ±45° to ±30° was a major improvement, as predicted by Scott Tyo [1] and Carl Baum [2]. This modification increases the effective gain (standard antenna gain minus return loss) and it dramatically reduces the cross-polarized effective gain.

Addition of the ground plane improved the mechanical properties of the antenna and improved the average crosspol rejection by 3 to 6 dB, depending on the specific versions of IRA-2 and IRA-3 one compares. While the IRA-2 had high-voltage resistors while the IRA-3 had the improved load configuration, we believe that the load would make little difference to the crosspol rejection. When we added both a radome and absorber foam to the IRA-3 the crosspol rejection was reduced to approximately that of the IRA-2. One advantage of the ground plane in the IRA-3 and IRA-4 is that the feed cable that normally is attached to the feed point from the rear can now be connected from the front. This reduces the TDR reflections at the feed point, which improves the effective gain.

We also gained a better understanding of how to construct the feed point to maintain a reasonably flat TDR, thereby improving the high-frequency response. First, the length of the two 100-ohm coax cables must be exactly the same length. In addition, the connections at the feed point must be as short as possible. In the case where a ground plane is present, this can be difficult, but a small triangle of metal soldered to the center conductor of the coax can reduce the inductance and aid in the attachment of the conductor to the antenna ground plane.

Another major improvement was the development of an improved splitter, which greatly reduced TDR reflections. As with the feed point, it is critical to use very short lengths of the center conductor to make the connection inside the splitter. It is also important to use a dielectric material inside the splitter that matches the dielectric constant of the insulator in the coax. We have also reduced the TDR reflections at the feed point and resistors. Reducing the reflections should improve the usefulness of IRAs for radar applications.

Table 1. Summary of IRA Measurements.

IRA Number	Feed Arm Angle	Load Configuration	Dummy Cables	Radome	Absorber Foam	Included in this report	Peak Gain		Height	Impulse, $h_N(t)$		Crosspol Rejection	
							Gain	Frequency	h_a	Peak	FWHM	Min.	Ave.
							dBi	GHz	mm	m/ns	ps	dB	dB
IRA-1-0	±45°	HVR					24.1	15	111	4.3	35.8	0.0	6.8
	±45°	Distributed					24.0	13	119	4.1	39.2	4.0	15.0
	±45°	Distributed	■			■	25.4	14	124	4.7	35.6	3.9	15.0
IRA-2-0	±30°	HVR				■	27.0	15	133	5.5	33.5	16.8	21.6
IRA-2-4	±30°	HVR					28.0	17	140	5.8	32.8	9.0	21.6
IRA-3-0	±30°	Inductive					25.8	16	124	5.1	34.0	13.7	27.6
	±30°	Inductive	■				27.8	15	131	5.7	32.8	18.5	28.0
	±30°	Inductive	■			■	26.5	14	139	5.4	35.5	4.1	24.0
	±30°	Inductive	■	■		■	25.6	17	139	4.9	37.2	7.5	23.0
	±30°	Inductive	■	■	■	■	24.7	14	112	4.2	36.2	1.6	20.3
IRA-3-1	±30°	Inductive					27.0	16	128	5.2	34.7	13.0	30.0
	±30°	Inductive	■				25.0	14	130	4.8	36.7	7.7	23.8
IRA-3-2	±30°	Inductive					27.3	12	126	5.0	34.8	0.0	23.0
	±30°	Inductive			■		22.7	12	110	3.9	37.5	0.0	20.3
	±30°	Inductive	■				25.6	15	139	5.0	36.6	0.0	19.5
	±30°	Inductive	■		■		24.3	15	120	4.2	35.6	0.0	21.7
IRA-4-0	±30°	Inductive				■	24.7	12	110	4.1	37.4	4.0	18.8
	±30°	Inductive			■		24.0	14	104	4.5	34.7	0.0	18.5
	±30°	Inductive	■			■	25.0	13	118	4.5	36.6	0.0	20.4
	±30°	Inductive	■		■	■	25.0	14	108	4.3	34.8	0.0	17.2

V. Conclusions.

Based on our experiments, we are able to make specific recommendations for improvements in the IRA design. By placing the feed arms at ±30° to vertical, we increased gain and reduced crosspol. By a variety of adjustments, we were able to reduce significantly the TDR reflections from three points on the antenna; the splitter, the feed point, and the resistors. This feature may be important in radar applications, which require low reflections. By including a ground plane, we reduced the crosspol and increased the mechanical strength of the antenna. We have also tested a radome for the antenna built by MRC, which seems to provide good protection to the outside of the antenna with minimal transmission loss.

We also tried several adjustments that did not help as much as we had hoped. We found that dummy cables added to maintain symmetry do not help very much in reducing crosspol. In addition, we were unable to reduce the sidelobes by reducing the fields near the rim of the reflector. We tried this both by moving the feed arms closer to the center of the reflector, and by adding absorber foam. It is possible that a thicker foam might be effective, but this may not be practical.

Of the four antennas we studied, it appears that the IRA-3 is the preferred configuration for most situations. The IRA-1 has lower gain than the IRA-3, with comparable reflection losses at the resistors. The IRA-2 has a higher crosspol than the IRA-3, and it is slightly less sturdy. The IRA-4 has slightly lower gain than the IRA-3, with higher crosspol and sidelobes.

References

1. J. S. Tyo, Optimization of the Feed Impedance for an Arbitrary Crossed-Feed-Arm Impulse Radiating Antenna, Sensor and Simulation Note 438, November 1999.

2. C. E. Baum, Selection of Angles Between Planes of TEM Feed Arms of an IRA, Sensor and Simulation Note 425, August 1998.

3. L. H. Bowen, E. G. Farr, C. E. Baum, T. C. Tran, and W. D. Prather, Experimental Results of Optimizing the Location of Feed Arms in a Collapsible IRA and a Solid IRA, Sensor and Simulation Note 450, November 2000.

4. L. H. Bowen, E. G. Farr, W. D. Prather, An Improved Collapsible Impulse Radiating Antenna, Sensor and Simulation Note 444, April 2000.

5. E. G. Farr and C. E. Baum, Time Domain Characterization of Antennas with TEM Feeds, Sensor and Simulation Note 426, October 1998.

6. L. H. Bowen, E. G. Farr, and W. D. Prather, "A Collapsible Impulse Radiating Antenna," in A. Stone (ed.) Ultra-Wideband, Short-Pulse Electromagnetics 5, Kluwer, (in publication), (proceedings of the 2000 EUROEM conference held in Edinburgh, June 2000).

7. C. E. Baum, Symmetry in Single-Polarization Reflector Impulse Radiating Antennas, Sensor and Simulation Note 448, July 2000.

8. J. S. Tyo, Personal communication.

9. E. G. Farr, L. H. Bowen, G. R. Salo, J. S. Gwynne, C. E. Baum, W. D. Prather, and T. Tran, Studies of an Impulse Radiating Antenna and a Pulse Radiating Antenna Element for SAR and Target Identification Applications, Sensor and Simulation Note 442, March 2000.

10. C. E. Baum, Some Topics Concerning Feed Arms of Reflector IRAs, Sensor and Simulation Note 414, October 1997.

11. M. Abdallah, M. Skipper, D. V. Giri, *et al*, Evaluation of the Terminating Impedance in the Conical-Line Feed of the 6-foot IRA, Prototype IRA Memo 8, April 2001.

12. D.V. Giri and C.E. Baum, Field Containing Solenoidal Inductors, Sensor and Simulation Note 368, July 1994.

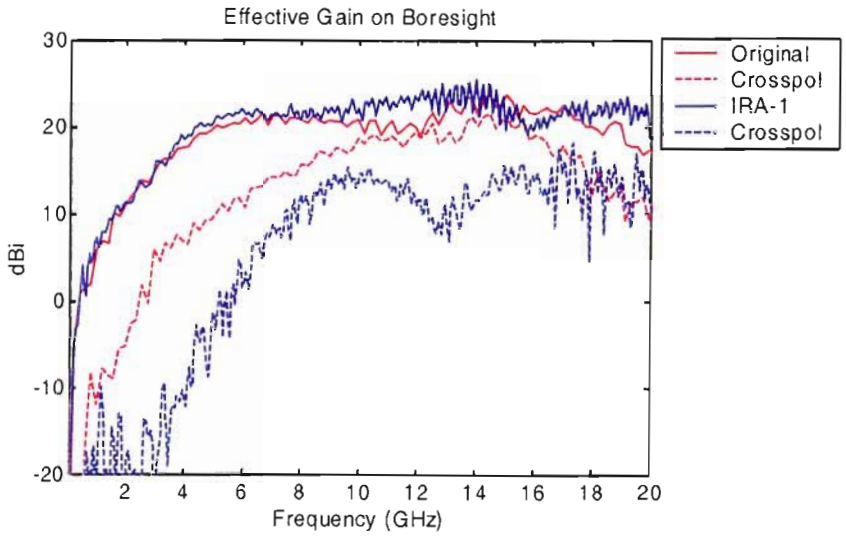

Figure 2.5. Comparison of the original and improved IRA-1.

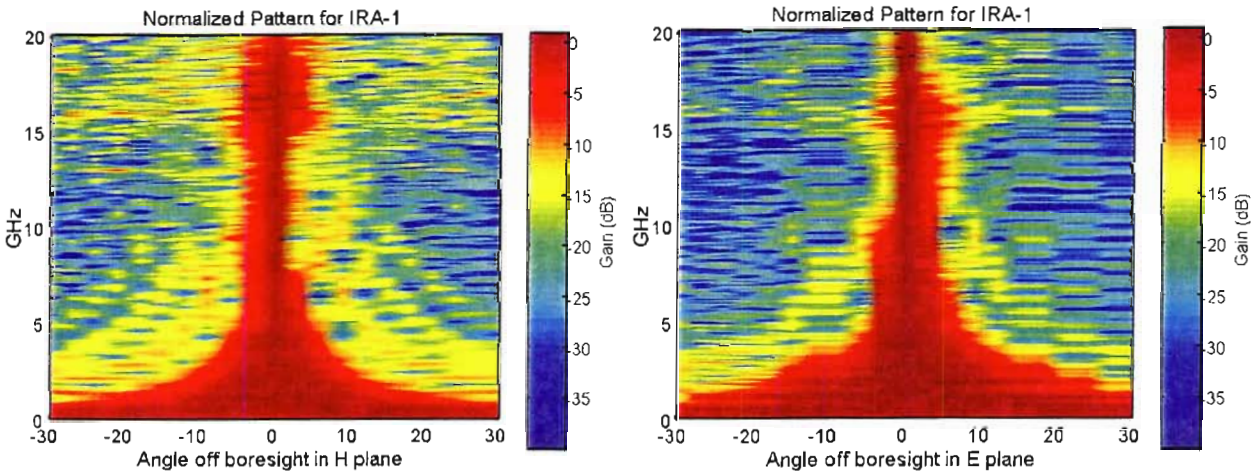

Figure 2.6. Normalized antenna pattern for the IRA-1. Angle is in degrees.

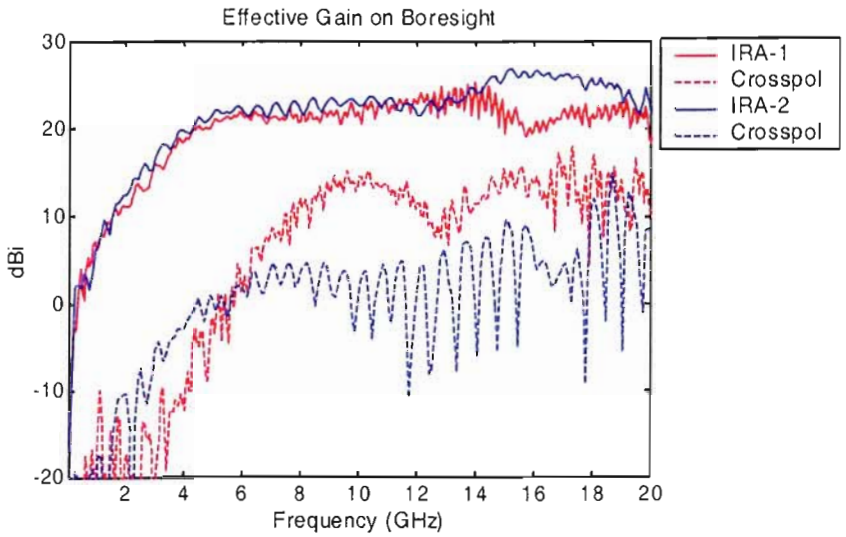

Figure 3.5. Comparison of IRA-1 and IRA-2 including crosspol.

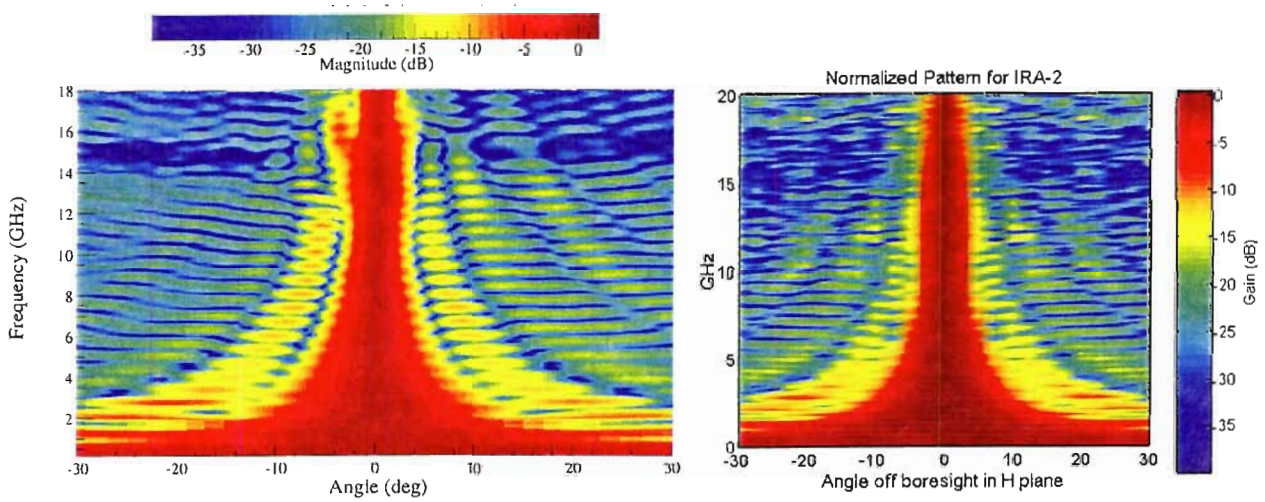

Figure 3.6. Pattern of the IRA-2 in the H plane, MRC left, FRI right. Angle is in degrees.

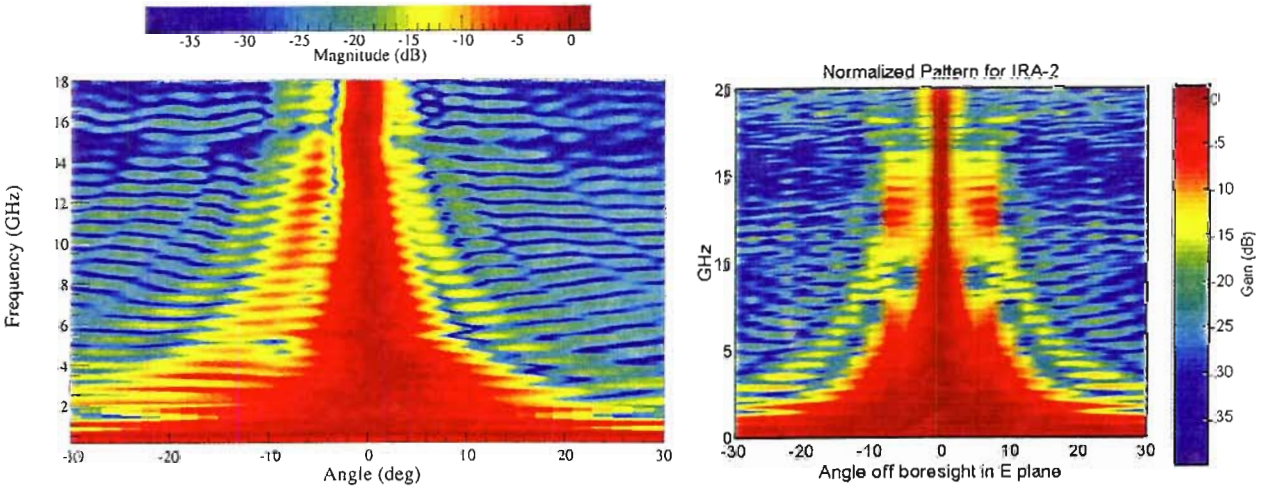

Figure 3.7. Pattern of the IRA-2 in the E plane, MRC left, FRI right. Angle is in degrees.

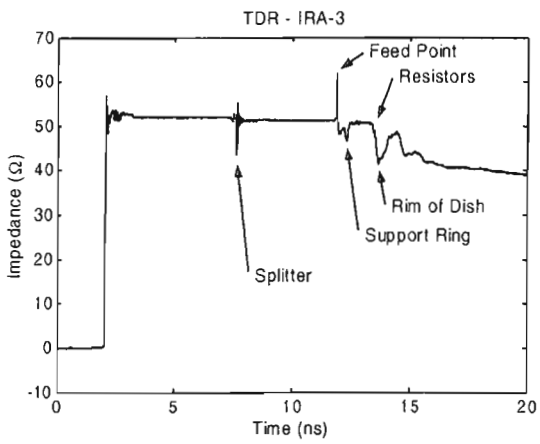

Figure 4.6. TDR with dummy cables.

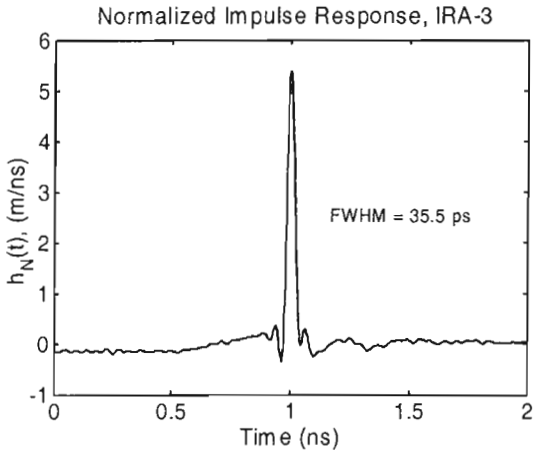

Figure 4.7. Normalized Impulse Response.

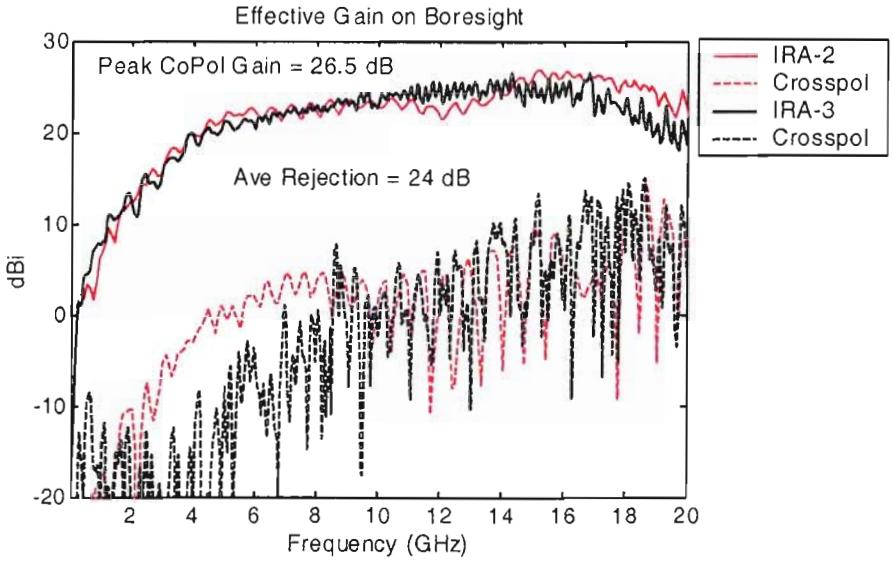

Figure 4.8. Effective Gain on Boresight of the IRA-3 with the IRA-2 included for comparison.

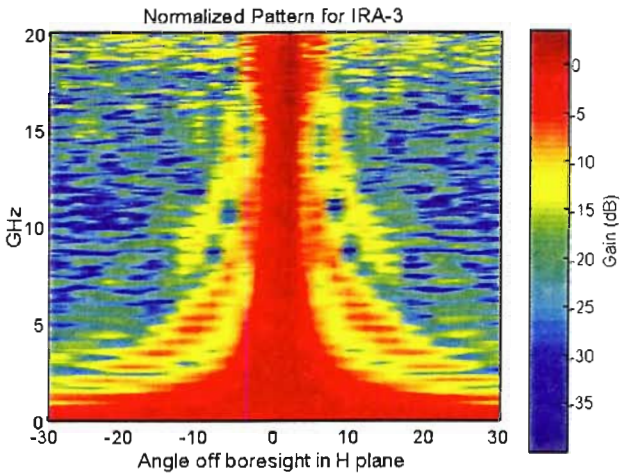

Figure 4.9. Pattern in the H plane. Angle is in degrees.

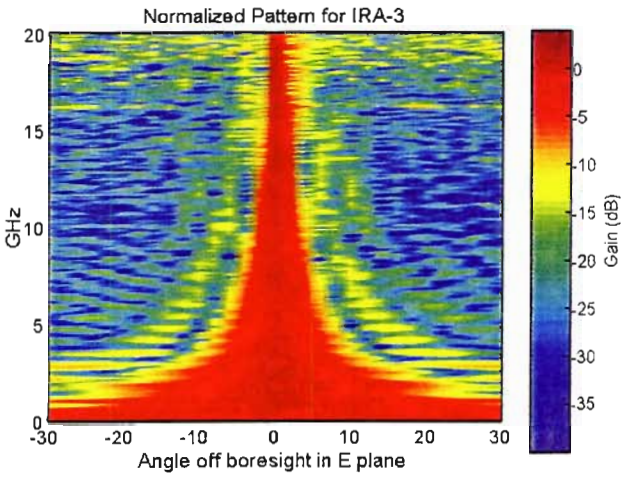

Figure 4.10. Pattern in the E plane. Angle is in degrees.

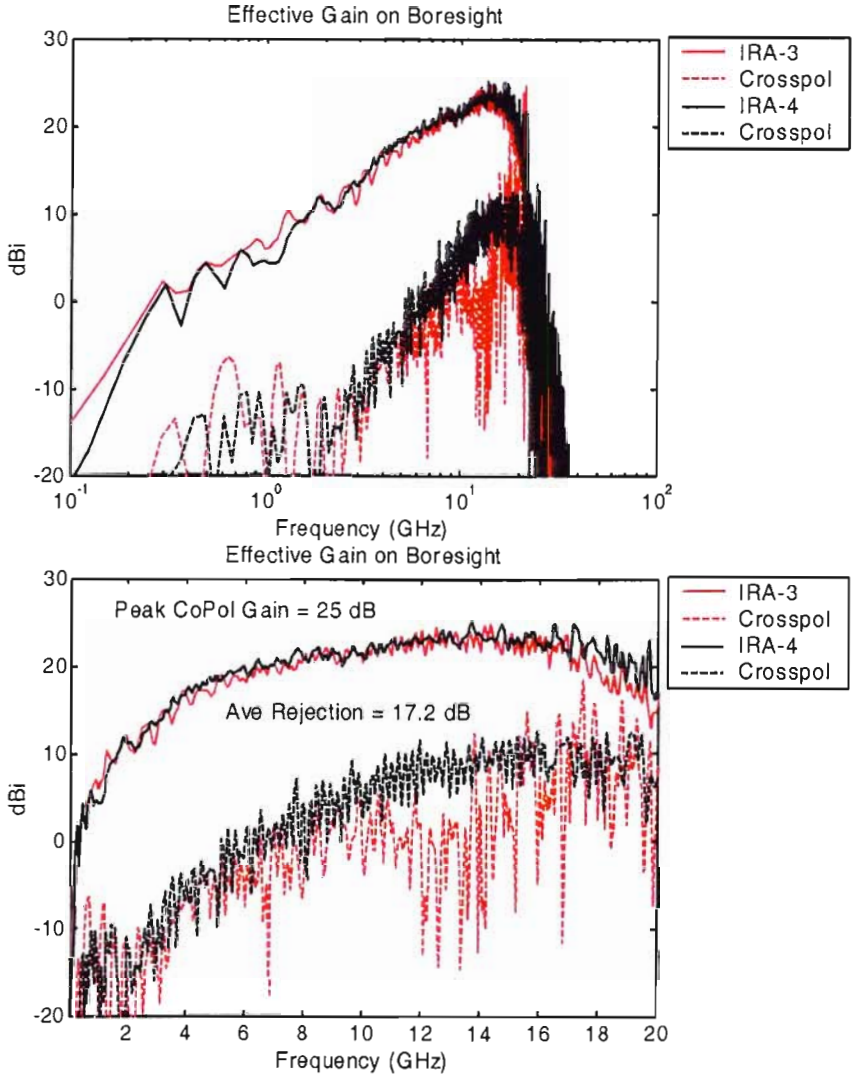

Figure 5.17. Comparison of the effective gain of the IRA-4 and the IRA-3 (from Figure 4.20)

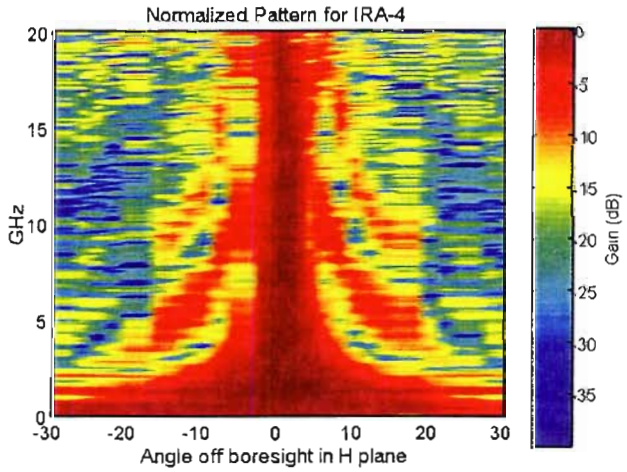

Figure 5.18. Pattern in the H plane. Angle is in degrees.

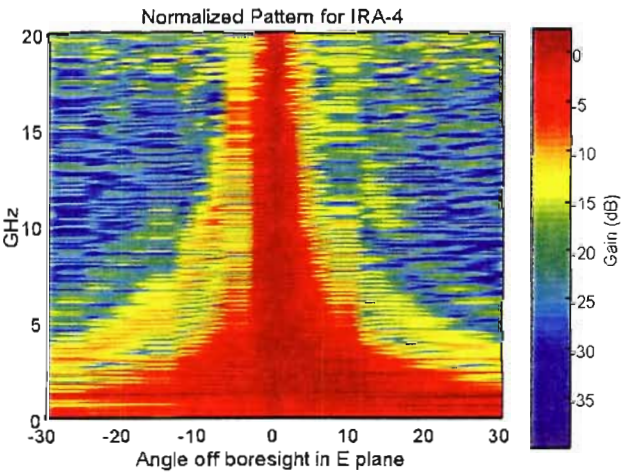

Figure 5.19. Pattern in the E plane. Angle is in degrees.

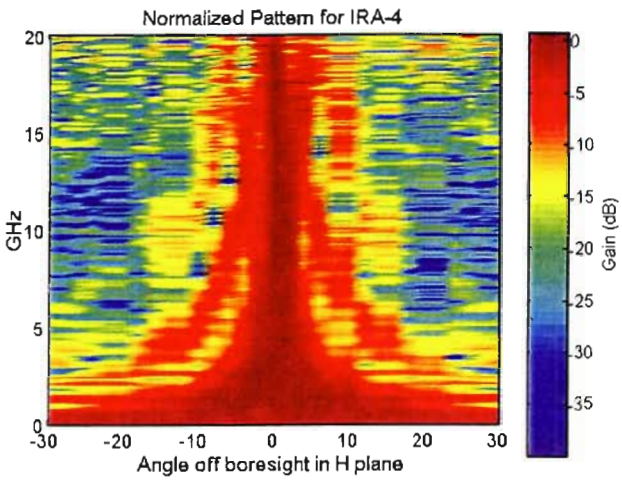

Figure 5.12. Pattern in the H plane. Angle is in degrees.

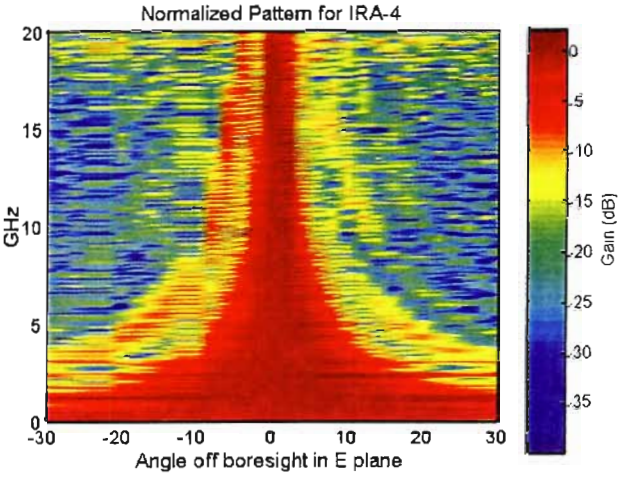

Figure 5.13. Pattern in the E plane. Angle is in degrees.

For a final comparison, we add absorber foam around the rim of the reflector dish on the IRA-4. The ¾-inch thick foam, shown in Figure 5.14, is designed for use at frequencies above 3.5 GHz. Between the feed arms we extended the foam to cover the area where the electric field has the incorrect polarity. This is a larger area than that of the IRA-3. Covering this area should improve the gain of the antenna.

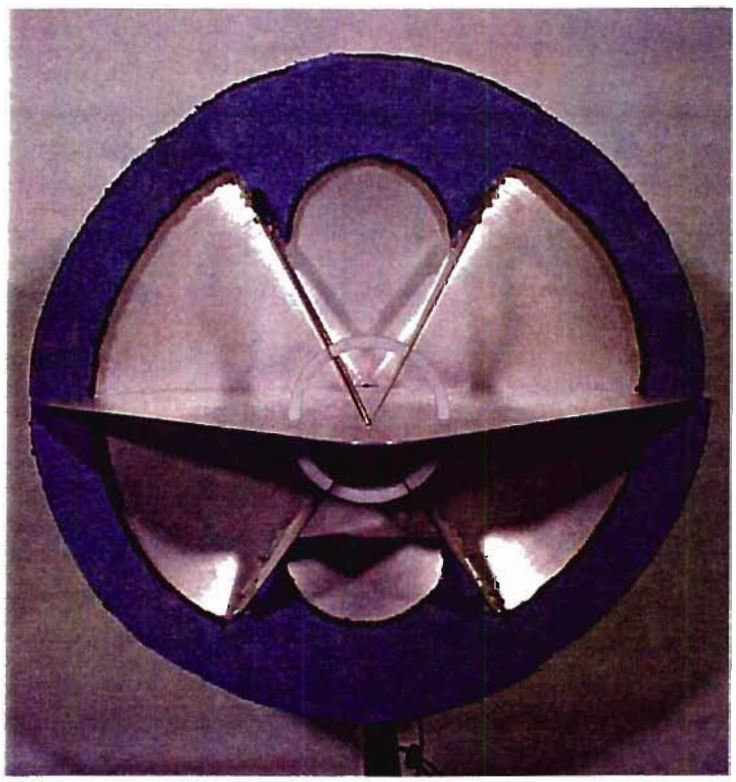

Figure 5.14. IRA-4 with absorber foam around rim.

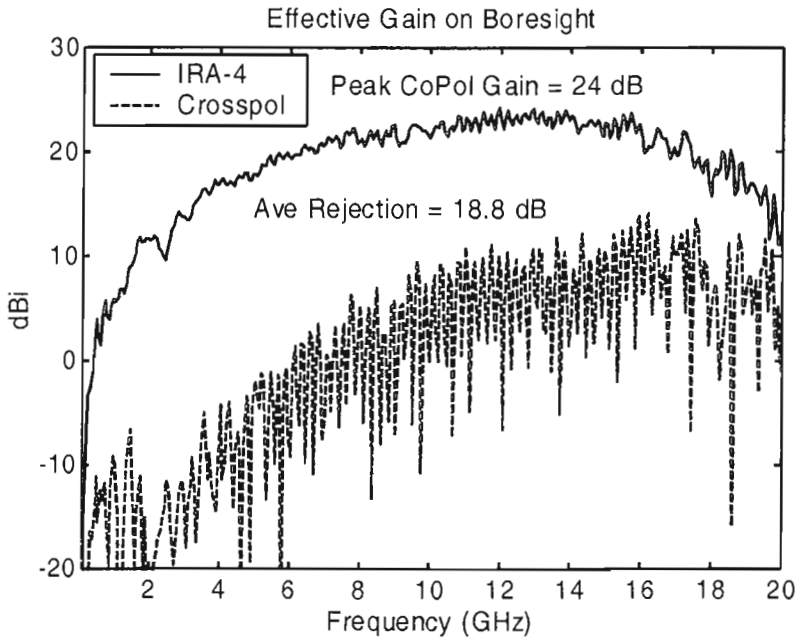

Figure 5.5. Effective gain of the IRA-4.

The patterns in the H and E planes are shown in Figures 5.6 and 5.7. Recall that the goal of this design was to reduce the sidelobes. However, in the H plane the sidelobes are quite pronounced, so moving the feed arms closer to the center does not seem to help.

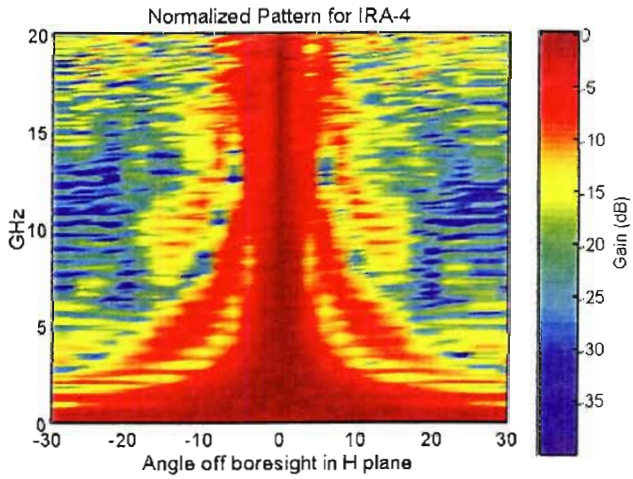

Figure 5.6. Pattern in the H plane. Angle is in degrees.

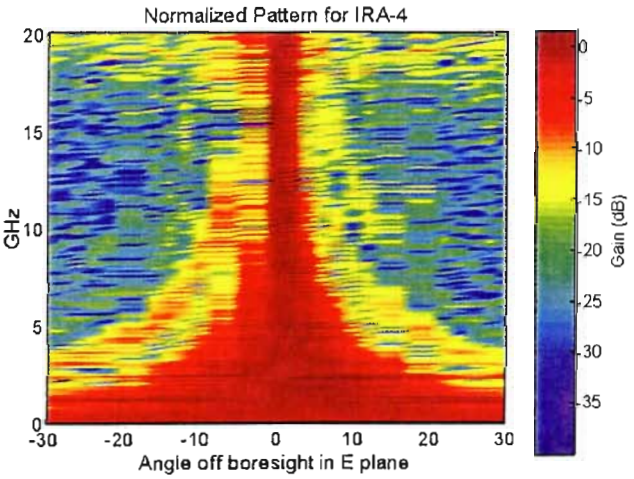

Figure 5.7. Pattern in the E plane. Angle is in degrees.

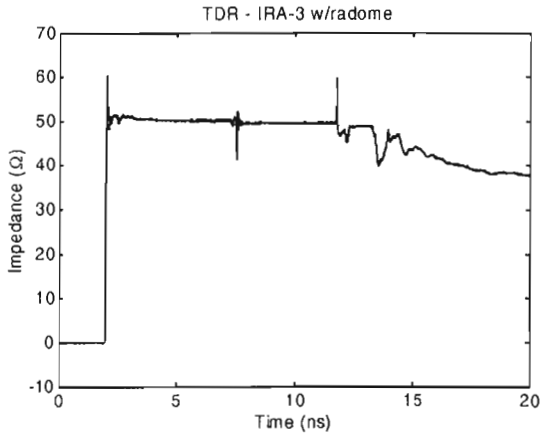

Figure 4.12. TDR of IRA-3 with radome.

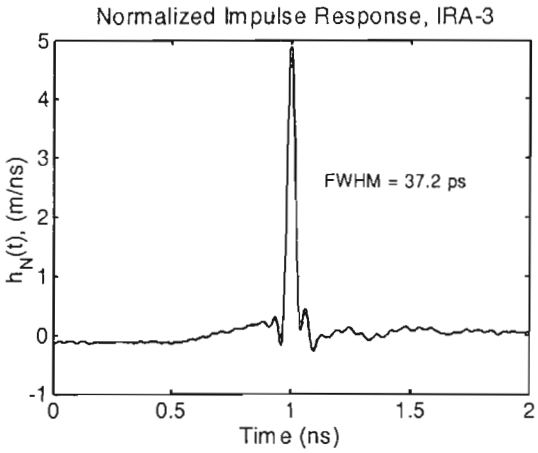

Figure 4.13. Normalized Impulse Response.

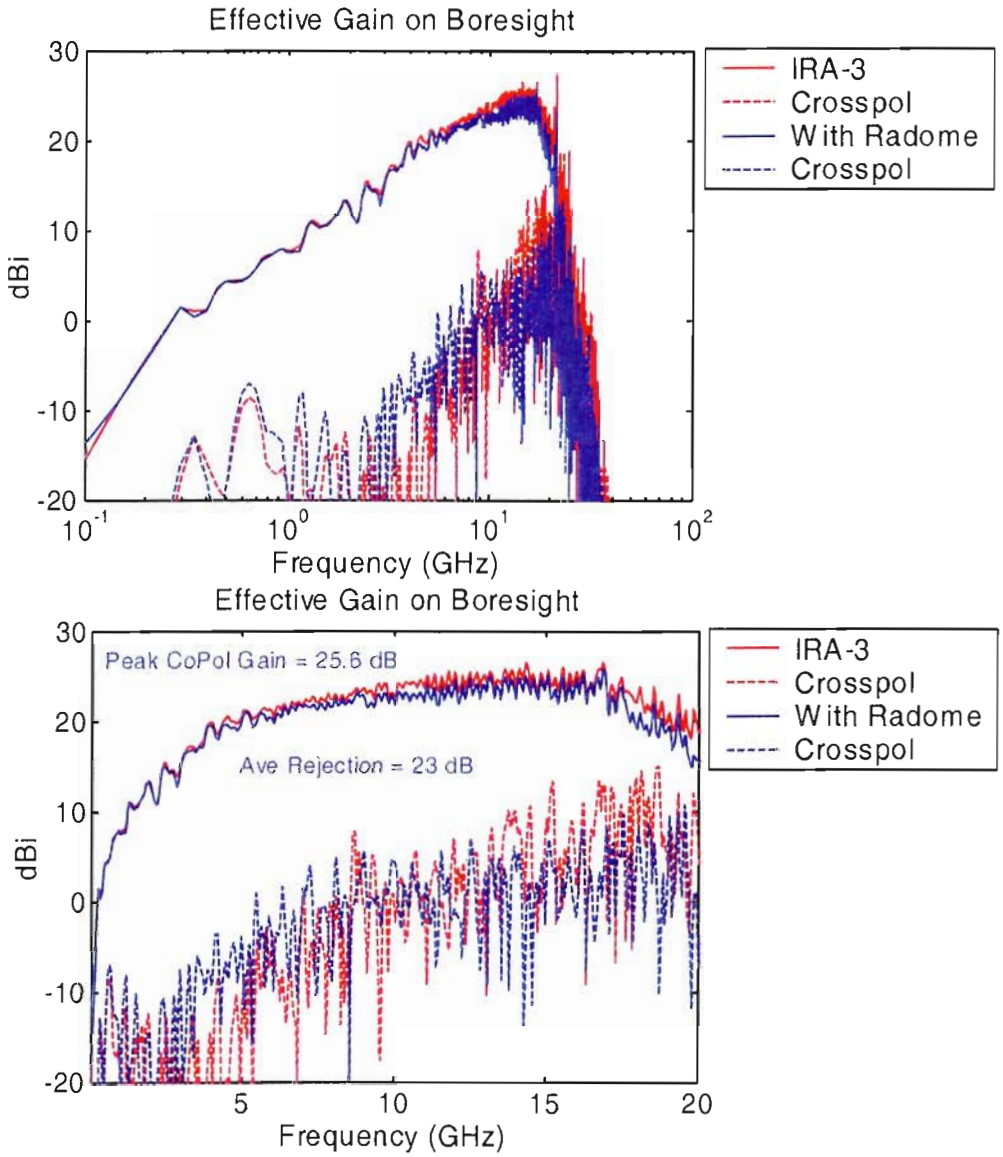

Figure 4.14. Effective gain of the IRA-3 with and without the radome.

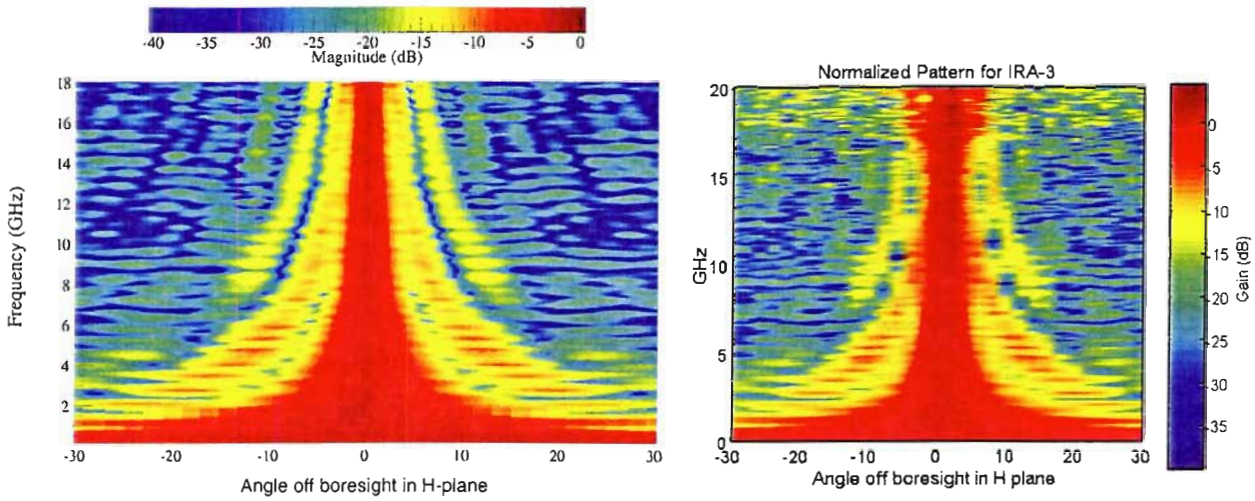

Figure 4.15. Pattern of the IRA-3 in H plane, MRC left, FRI right. Angle is in degrees.

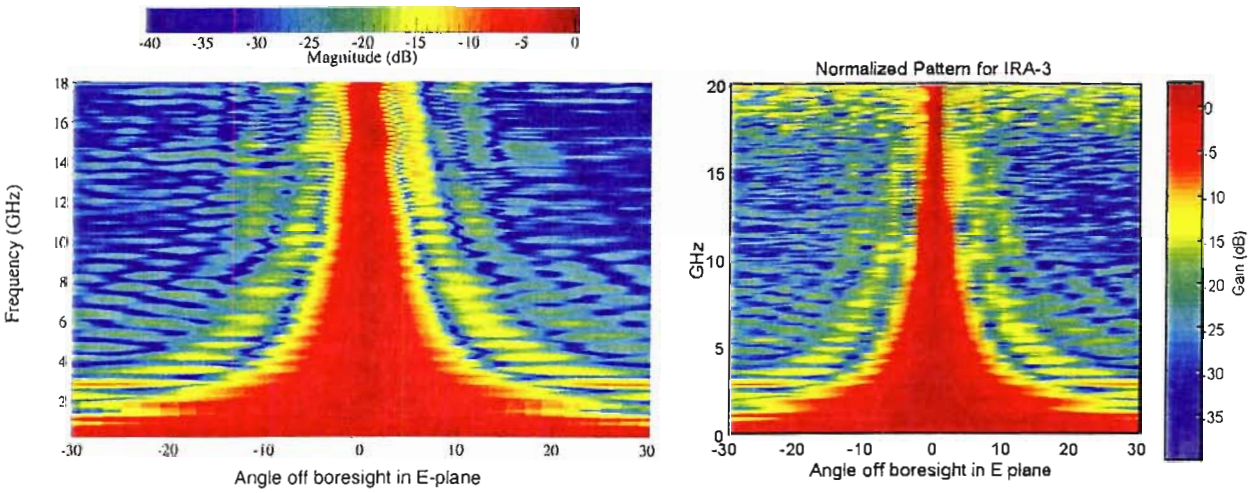

Figure 4.16. Pattern of the IRA-3 in the E plane, MRC left, FRI right. Angle is in degrees.

The last modification to the IRA-3 was the addition of absorber foam around the rim of the reflector dish. The foam was intended to reduce the fields near the edge of the reflector, and to reduce the E field in areas where the polarity is reversed. The IRA-3 with the foam in place is shown in Figure 4.17. The foam was 1.125 inches thick, and according to the manufacturer, this foam is designed for use at frequencies above 2.5 GHz. The foam extends over the portion of the reflector between the feed arms where the E field has the incorrect polarity. The radome was replaced before making the measurements reported below.

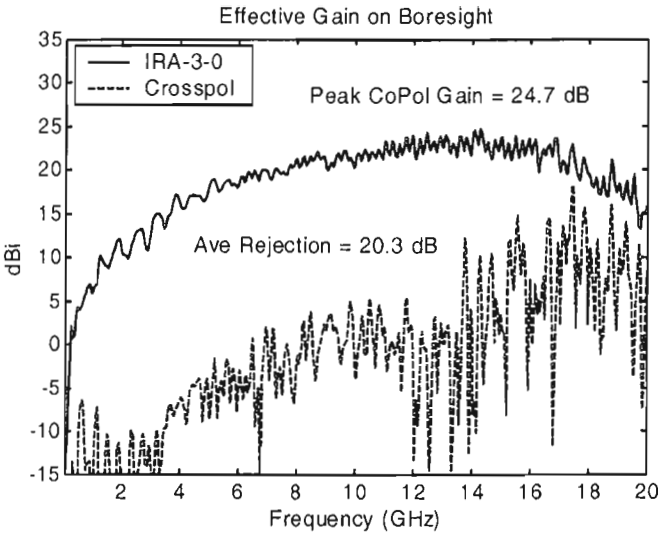

Figure 4.20. Effective gain of the IRA-3 with radome and absorber foam.

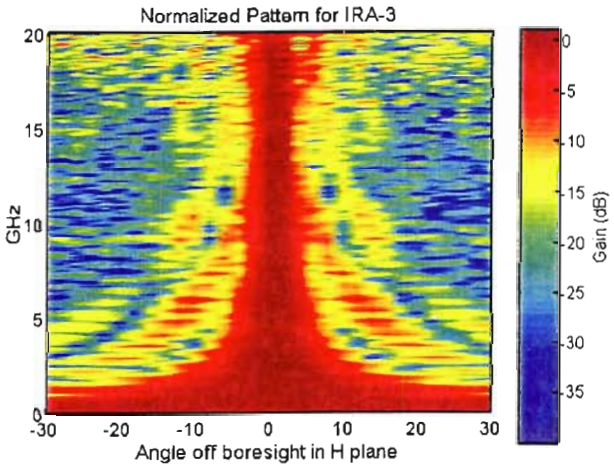

Figure 4.21. Pattern in the H plane. Angle is in degrees.

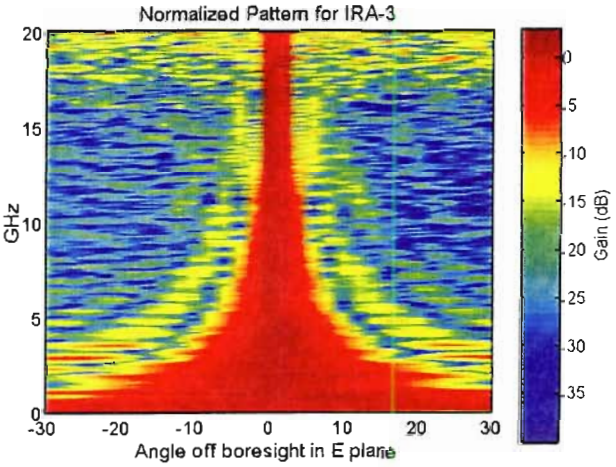

Figure 4.22. Pattern in the E plane. Angle is in degrees.

As a result of our studies on the IRA-3, we have learned a number of things. We have found that adding a ground plane reduces crosspol and makes the antenna more sturdy. We found a configuration of metal-film resistors that reduces reflections at the ends of the feed arms. We found that feeding the antenna from the front provides lower TDR losses at the feed point. We found that dummy cables do not reduce crosspol appreciably. We found that adding foam does not reduce sidelobes. Finally, we found that adding a radome seems to affect performance very little. We next turn our attention to the IRA-4.